

USE OF SENSITIVITY AND UNCERTAINTY ANALYSIS IN THE DESIGN OF REACTOR PHYSICS AND CRITICALITY BENCHMARK EXPERIMENTS FOR ADVANCED NUCLEAR FUEL

FISSION REACTORS

KEYWORDS: *sensitivity and uncertainty analysis, experiment design, highly enriched fuel*

B. T. REARDEN *Oak Ridge National Laboratory, P.O. Box 2008
Oak Ridge, Tennessee 37831-6170*

W. J. ANDERSON *Framatome ANP, Inc., P.O. Box 10935, 3315 Old Forest Road
Lynchburg, Virginia 24506-0935*

G. A. HARMS *Sandia National Laboratories, P.O. Box 5800
Albuquerque, New Mexico 87185-1146*

Received June 4, 2004

Accepted for Publication September 14, 2004

Framatome ANP, Sandia National Laboratories (SNL), Oak Ridge National Laboratory (ORNL), and the University of Florida are cooperating on the U.S. Department of Energy Nuclear Energy Research Initiative (NERI) project 2001-0124 to design, assemble, execute, analyze, and document a series of critical experiments to validate reactor physics and criticality safety codes for the analysis of commercial power reactor fuels consisting of UO_2 with ^{235}U enrichments ≥ 5 wt%. The experiments will be conducted at the SNL Pulsed Reactor Facility.

Framatome ANP and SNL produced two series of conceptual experiment designs based on typical param-

eters, such as fuel-to-moderator ratios, that meet the programmatic requirements of this project within the given restraints on available materials and facilities. ORNL used the Tools for Sensitivity and Uncertainty Analysis Methodology Implementation (TSUNAMI) to assess, from a detailed physics-based perspective, the similarity of the experiment designs to the commercial systems they are intended to validate. Based on the results of the TSUNAMI analysis, one series of experiments was found to be preferable to the other and will provide significant new data for the validation of reactor physics and criticality safety codes.

I. INTRODUCTION

Framatome ANP, Sandia National Laboratories (SNL), Oak Ridge National Laboratory (ORNL), and the University of Florida (UF) are collaborating on the U.S. Department of Energy Nuclear Energy Research Initiative (NERI) project 2001-0124 to design, assemble, analyze, and document a series of critical experiments to validate reactor physics and criticality safety codes for the analysis of commercial pressurized water reactor

(PWR) and boiling water reactor (BWR) UO_2 fuels with ^{235}U enrichments ≥ 5 wt%.

At the inception of this project, a supply of nuclear fuel, originally manufactured for the PATHFINDER system intended for assembly at The Pennsylvania State University (Penn State) in the 1960s, was identified for use in the experiments. The PATHFINDER program was eventually canceled; the fuel was never irradiated and has been in storage at Penn State for many years. For this current project, the PATHFINDER fuel has been shipped to SNL for disassembly. Disassembly is necessary because the PATHFINDER fuel is ~ 2 m long and bundled

*E-mail: reardenb@ornl.gov

in hexagonally pitched assemblies. The fuel pellets will be removed from their existing cladding and placed in a new cladding of the appropriate length to meet the needs of this program. The PATHFINDER fuel consists of sintered UO_2 pellets with an enrichment of 6.93 wt% ^{235}U and a diameter of 0.526 cm (Ref. 1).

The critical assembly comprising the 6.93 wt% fuel will be operated within the SNL Pulse Reactor Facility (SPRF) with the reactor room as the primary structure for housing the assembly during operation. These are the same core tank, control systems, and reactor room recently used for the NERI-sponsored Burnup Credit Critical Experiment² (BUCCX).

FRAMATOME ANP developed two series of conceptual experimental designs within the programmatic restraints of the project. Both series of experiments are representative of PWR and BWR fuel-to-moderator and metal-to-moderator ratios and maintain consistency between experiment geometry and current capabilities of PWR and BWR analysis tools used for reload designs. The conceptual experiment designs consist of fuel rods composed of PATHFINDER pellets in aluminum cladding with a fuel height of 50 cm. The fuel rods are to be assembled in symmetric square-pitched lattices and fully flooded in an open tank with borated water, such that the experiment geometry will be suitable for modeling with commercial reactor physics codes. Criticality will be achieved by diluting the boron concentration in the water moderator. Each series of experiments has different arrangements of the fuel rods. Within each series of similar experiments, differing fuel rod pitches, temperatures, and $\text{UO}_2\text{-Gd}_2\text{O}_3$ -fueled burnable absorber rods will be investigated.

ORNL used the Tools for Sensitivity and Uncertainty Analysis Methodology Implementation^{3,4} (TSUNAMI) from the SCALE code system⁵ to assess the similarity of conceptual experiment designs to the intended commercial applications. TSUNAMI includes one-dimensional and three-dimensional sensitivity analysis sequences that compute the sensitivity of k_{eff} to the neutron cross-section data. These sensitivity data can be used to compute relational integral indices that assess the similarity of two systems based on the nuclide-reaction-specific and energy-dependent sensitivity data. TSUNAMI has been demonstrated as an effective method for determining the applicability of benchmark experiments for use in code validation.⁶

This paper is organized as follows. A number of prototypic commercial fuel designs using highly enriched UO_2 fuels are described in Sec. II. These fuels serve as the basis for the assessment of the applicability of the proposed experiments, which are described in Sec. III, and existing experiments, which are described in Sec. IV. The TSUNAMI techniques used to assess the applicability of the existing and proposed experiments to the prototypic commercial fuel designs are described in Sec. V. The results of the TSUNAMI analyses for the existing

and proposed experiments to the prototypic commercial fuel designs are presented in Secs. VI and VII, respectively, and a more detailed evaluation of one proposed experiment is presented in Sec. VIII. Finally, conclusions are presented in Sec. IX.

II. PROTOTYPIC COMMERCIAL FUEL DESIGNS

Representative fuel assemblies of widely used commercial power reactor fuels were selected for analysis in this study. The applicability of the proposed experiments to the code validation of these assemblies is addressed in Secs. VII. These representative assemblies are selected to show trends in the data with regard to the applicability of experiments to existing commercial reactor designs. Additional fuel designs may be considered in future analyses, as needed, to represent future designs using highly enriched fuel.

Three commercial fuel designs were considered in this study: the Babcock and Wilcox (B&W) 15×15 fuel assembly, the Westinghouse 17×17 fuel assembly, and the General Electric (GE) 8×8 fuel assembly. The configurations of the assemblies are shown in Figs. 1, 2, and 3, respectively, and some properties of the assemblies are shown in Table I. In each assembly, the fuel is UO_2 at 96% of theoretical density or 10.5216 g/cm^3 .

Each of the assemblies shown in Table I was modeled with ^{235}U enrichments of 4, 6, 7, and 10 wt%.

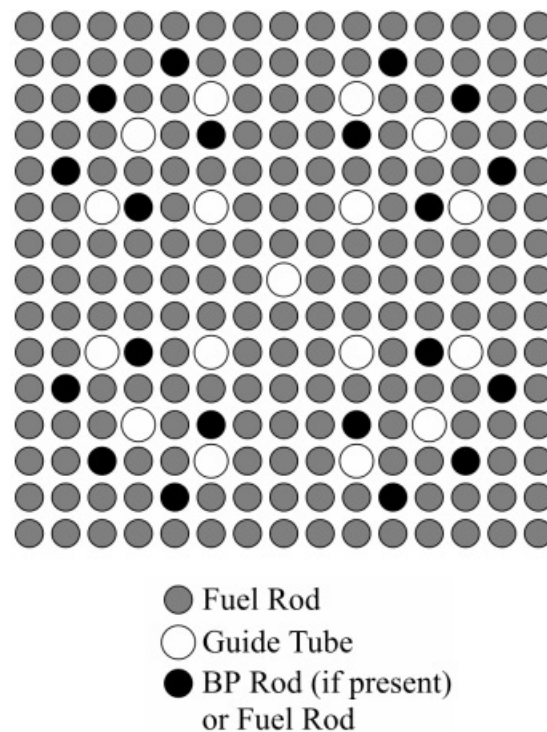


Fig. 1. Configuration of B&W assembly.

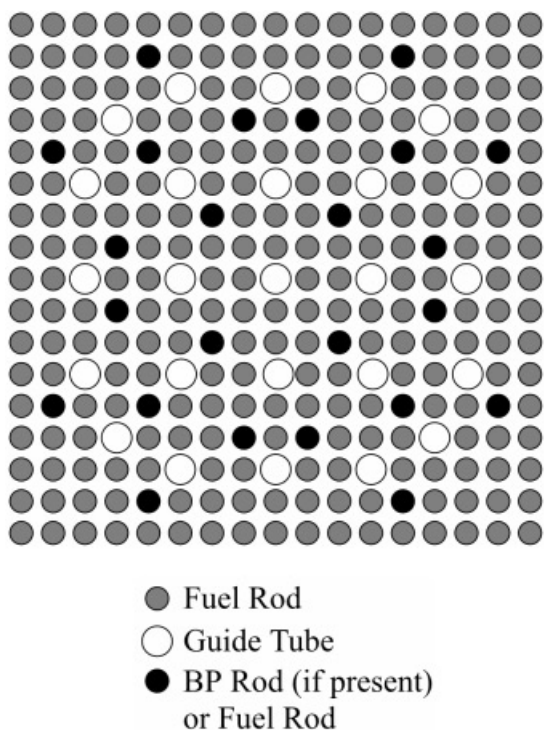


Fig. 2. Configuration of Westinghouse assembly.

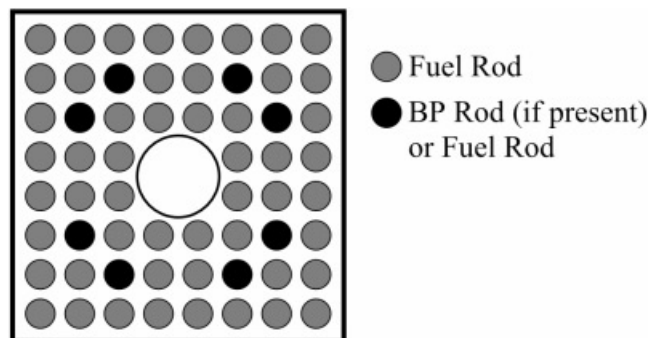


Fig. 3. Configuration of GE assembly.

Furthermore, each configuration was modeled under various conditions that could be encountered throughout the fuel cycle, excluding burnup. Each design was modeled at two temperatures. Shipping, storage, and initial core loading conditions were simulated with models at 20°C. Average properties at operating conditions were modeled at higher temperatures. The same conditions were used for all low-temperature models of the various fuel types. At the high temperature, the same average properties were used for the PWR fuel types (i.e., B&W and Westinghouse), and different conditions were considered for the BWR fuel (i.e., GE). For the BWR fuel, a uniform average moderator density was used. The temperature and moderator density conditions used in the models are shown in Table II.

Burnable poison (BP) rods were also considered in the commercial fuel models. For all fuel types and enrichments, the BP rods were composed of Gd_2O_3 in UO_2 with 4 wt% Gd_2O_3 and a ^{235}U enrichment of 4 wt%. The BP rods had the same dimensions as the fuel rods they replace in each model and were modeled at the same temperatures as the fuel rods. The number of poison rods for each assembly type was as follows: B&W 15×15 had 20 BPs, Westinghouse 17×17 had 24 BPs, and GE 8×8 had 8 BPs. The loading patterns for the BP rods were based on those commonly used for the specific fuel types and are shown in Figs. 1, 2, and 3.

All commercial fuel assembly models were reflected on the x and y boundaries to create infinite arrays. Most models consist of one assembly with the appropriate interstitial assembly spacing and reflective boundary conditions. In some cases, a simulated core loading was produced with nine assemblies in a 3×3 array with three assemblies containing BPs and the other six with no BPs. For these cases, the three assemblies with BP rods were placed along the diagonal of the 3×3 array. The 3×3 array is reflected along the x and y boundaries to produce an infinite “core” with a one-third loading of BP assemblies. The BP grid arrangement is shown in Fig. 4. It is acknowledged that in an actual core design, the non-BP assemblies would be burned fuel. However, the goal of the one-third loading is to assess the importance of the

TABLE I
Design Properties of Commercial Fuel Assemblies Considered in This Study

Assembly	Fuel Outer Diameter (cm)	Clad Outer Diameter (cm)	Pitch (cm)	Fuel-to-Water Ratio	Clad Material
B&W 15×15	0.9505	1.0871	1.4427	0.6153	Zr
Westinghouse 17×17	0.7844	0.9144	1.2598	0.5194	Zr
GE 8×8	1.04394	1.2268	1.6256	0.5860	Zircaloy-2

TABLE II
Temperature and Moderator Density Conditions Used for Commercial Fuel Models

Assembly Type/Condition	T_{fuel} (°C)	T_{clad} (°C)	T_{mod} (°C)	ρ_{mod} (g/cm ³)
All/low temperature	20	20	20	0.99821
PWR/high temperature	577	322	284	0.7576
BWR/high temperature	567	347	285	0.5151

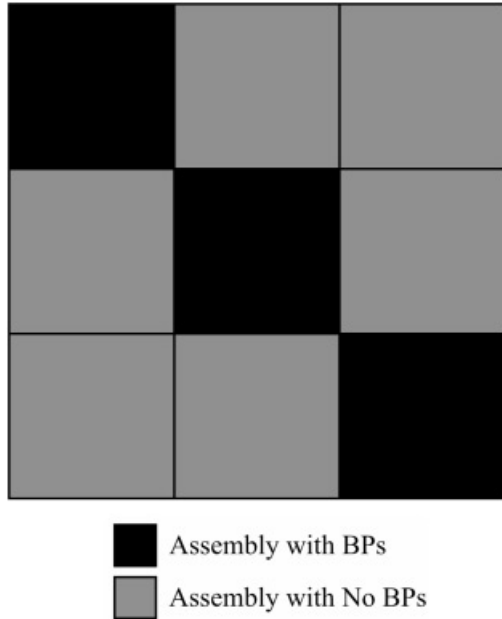


Fig. 4. Simulated core layout for BP grid configurations.

BP rods in a core, and this simplified model should adequately sample the BPs. The configurations modeled for each fuel assembly type are presented in Table III. In Table III, “All BP” indicates an infinite array of assem-

TABLE III
Assembly Configurations Modeled

Assembly	Low Temperature			High Temperature		
	All BP	BP Grid	No BP	All BP	BP Grid	No BP
B&W 15 × 15	✓	✓	✓	✓	✓	✓
Westinghouse 17 × 17			✓	✓		✓
GE 8 × 8	✓			✓		✓

blies with BPs, “BP Grid” indicates an infinite array of 3 × 3 clusters of assemblies where three of the nine assemblies contain BPs, and “No BP” indicates an infinite array of assemblies with no BPs. Each of these configurations was modeled for enrichments of 4, 6, 7, and 10 wt% ²³⁵U. Some of the PWR cases were modeled with 500-ppm natural boron in the moderator. The soluble boron was included in the low-temperature BP grid case and all high-temperature cases. Locations in Table III that do not contain check marks were not modeled and will appear as blank spaces in subsequent data tables.

III. PROPOSED EXPERIMENTS

Programmatic requirements described in Sec. I (e.g., 6.93 wt% fuel and BUCCX core tank) place restrictions on the design of experiments for this program. The two series of experimental designs developed by FRAM-ATOME ANP are described in this section. There are many common components in the two experiment designs. The primary difference between the two designs is the core loading pattern.

III.A. Equipment

The critical assembly will be operated within the SPRF with the reactor room as the primary structure for housing the assembly during operation. The same critical assembly and reactor room used for the NERI-sponsored BUCCX program² will also be used for this program. The control console will be housed in an ancillary building in the immediate vicinity of the reactor room. The inherent safety of the massive structure of the reactor room provides adequate protection from radiation exposure resulting from routine and anticipated abnormal operations. The reactor room also provides confinement ventilation with high-efficiency particulate air filtration of effluent.

The critical assembly will use the same hardware as the BUCCX critical assembly with the exception of a new core structure. New grid plates are necessary to accommodate the smaller-diameter fuel rods and a square-pitch array. The assembly consists of a tank with grid

plates, two safety elements, a control element, a neutron source, neutron detectors, and the associated safety channels. A superstructure above the tank supports the reactivity control drive mechanisms. The water moderator will be pumped from a tank below the level of the core tank. A dump valve for quick release of moderator provides a shutdown mechanism in addition to that achieved through the plant protection system.

These experiments will use the same tank as the BUCCX as shown in Fig. 5. The cylindrical tank is made of 6061 aluminum. The main part of the tank has a 93.68-cm inner diameter and is 102 cm tall. The walls are 0.64 cm thick, and the floor is 2.54 cm thick. The dimensions of the main section of the tank are sufficient to allow for an effectively infinite water reflector on all sides of the array (>15 cm). For the purposes of this

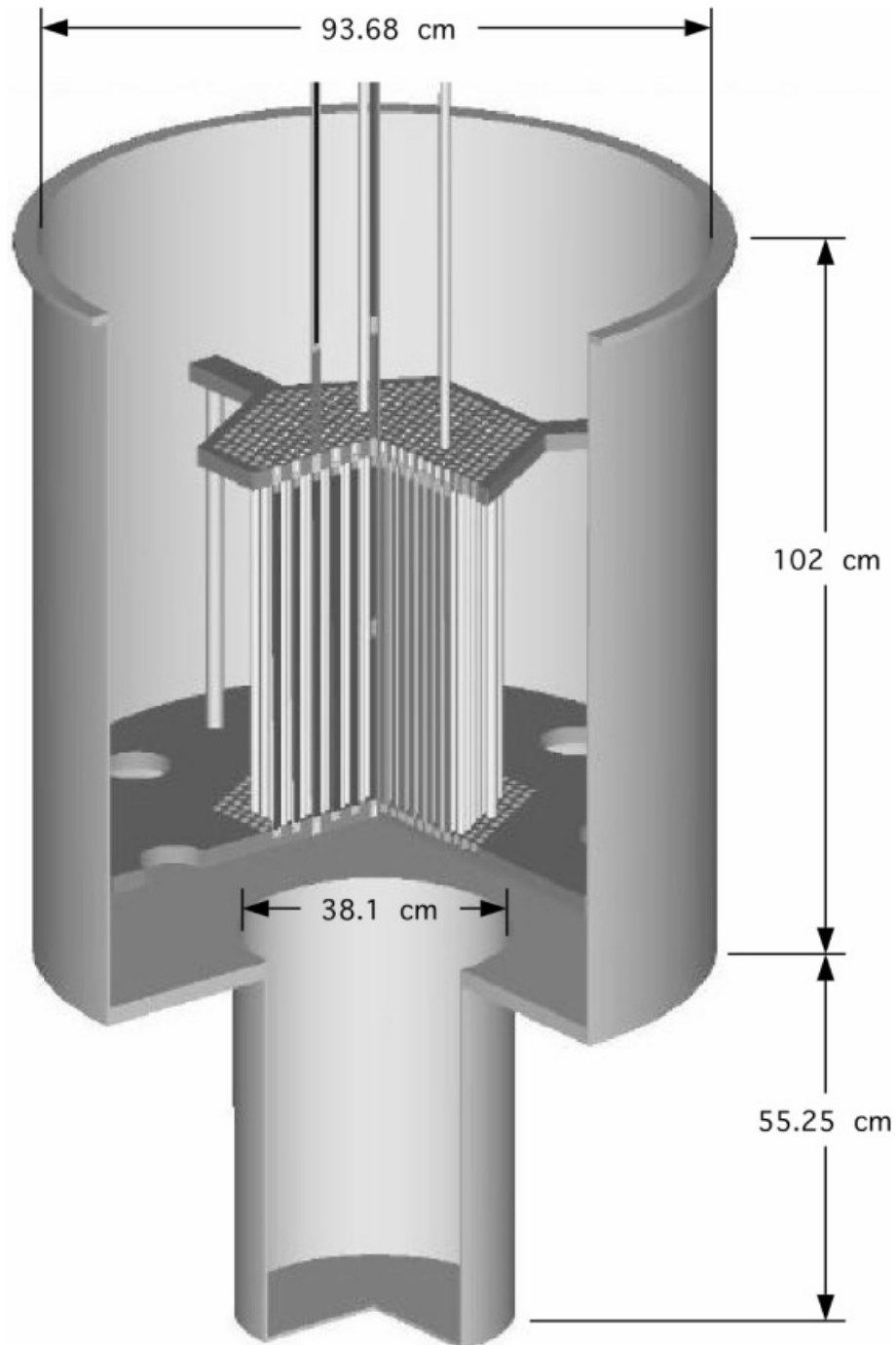


Fig. 5. Configuration of the critical assembly with water.

description, the inner surface of the bottom of the main part of the tank is considered the axial reference point (0.00 cm).

The fuel rods will be held in place during the experiments using upper and lower grid plates containing holes at the desired spacing. The grid plates will be made of 6061 aluminum. The holes for the fuel rods will be 0.660 cm in diameter. The bottom of the lower 2.54-cm-thick grid plate is located 15.24 cm above the axial reference point. The placement of the lower grid plate provides for an effectively infinite 15.24-cm-thick water reflector below the fuel.

The bottom of the 2.54-cm-thick upper grid plate is located at a height of 68.28 cm. A standpipe sets the maximum water level 15.24 cm above the top grid plate or at 86.06 cm with respect to the axial reference. The water level will be sufficient to provide an effectively infinite 15.24-cm-thick water reflector above the fuel.

The tank also includes a lower section, which was used in the BUCCX for the fuel-followed control rods when they were lowered though the experimental core. This lower section has an inner diameter of 38.10 cm. The inside of the projection goes down to -55.25 cm. The floor of the projection is 0.64 cm thick.

III.B. Fuel

The cylindrical fuel rods planned for these experiments consist of 0.0363-cm-thick 3003 aluminum clad, into which PATHFINDER uranium dioxide pellets (described in Sec. I) will be inserted to an active fuel length of ~ 50 cm. The outer diameter of the clad will be 0.635 cm. A spring located at the top of the fuel stack will maintain the axial compression of the fuel stack within the fuel rod. Top and bottom end caps also will be installed on each fuel rod.

III.C. Absorber Materials

A portion of each series of experiments will contain fueled BP absorber rods. The BP rods will use the same 3003 aluminum cladding as the fuel rods so that the rods will fit into the grid plates. The absorber material will be $\text{UO}_2\text{-Gd}_2\text{O}_3$ as found in current light water reactor (LWR) assemblies. It is expected that the $\text{UO}_2\text{-Gd}_2\text{O}_3$ pellets will use 4.0 wt% ^{235}U in UO_2 in a matrix with Gd_2O_3 . The Gd_2O_3 will constitute 4.0 wt% in the $\text{UO}_2\text{-Gd}_2\text{O}_3$. The gadolinia pellets will have the same basic geometry as the fuel pellets, with an outside diameter of 0.526 cm, and will be loaded to an active height of 50 cm.

III.D. Critical Configurations

Each critical configuration will consist of a symmetric square-pitched array of fuel rods that is fully flooded and reflected with water. The excess reactivity in the

critical assembly will be shimmed with soluble boron in the moderator.

It is desirable to produce a series of critical configurations using two fuel-rod pitches and two moderator temperatures. The fuel-rod-pitch values are chosen to encompass the range of water-to-fuel ratios currently found in U.S. LWRs. The fuel-rod-pitch values chosen for evaluation are 0.800 and 0.855 cm, which produce fuel-to-water ratios of 0.67 and 0.52, respectively. The temperatures are chosen based on the range of temperatures that the experimental facility can support. The low value of 20°C is the effective ambient temperature in the facility. The high value of 60°C is the maximum temperature that the system can sustain without modifications to the hardware. In addition to varying the temperature and pitch, the variations of experimental configuration will also include the use of absorber rods. This involves replacing 20 fuel rods with 20 $\text{UO}_2\text{-Gd}_2\text{O}_3$ BPs for each pitch and temperature state point. The details of the configurations to be included in an experimental series are given in Table IV.

Two models are considered for the basic experiment design from which the variations will be produced. The first series of experiments, called the square series, consists of nine 15×15 assemblies in a 3×3 square as shown in Fig. 6. The other series of experiments, called the cruciform series, consists of five 17×17 assemblies in a cruciform pattern with four 8×8 assemblies in the corners as shown in Fig. 7.

Both the square series of experiments and the cruciform series of experiments are suitable for modeling with reactor physics and criticality codes commonly used in the United States.

III.D.1. Square Experiment Series

For the square experiment series, the fuel rods will be arranged in a pattern that resembles nine 15×15 assemblies, with 21 nonfuel holes, in a 3×3 array.

TABLE IV
Planned Experimental Suites

Suite	Pitch (cm)	Absorber	T_{mod} ($^\circ\text{C}$)
1	0.800	None	20
		None	60
2	0.800	20 Gd rods in center assembly	20
		20 Gd rods in center assembly	60
3	0.855	None	20
		None	60
4	0.855	20 Gd rods in center assembly	20
		20 Gd rods in center assembly	60

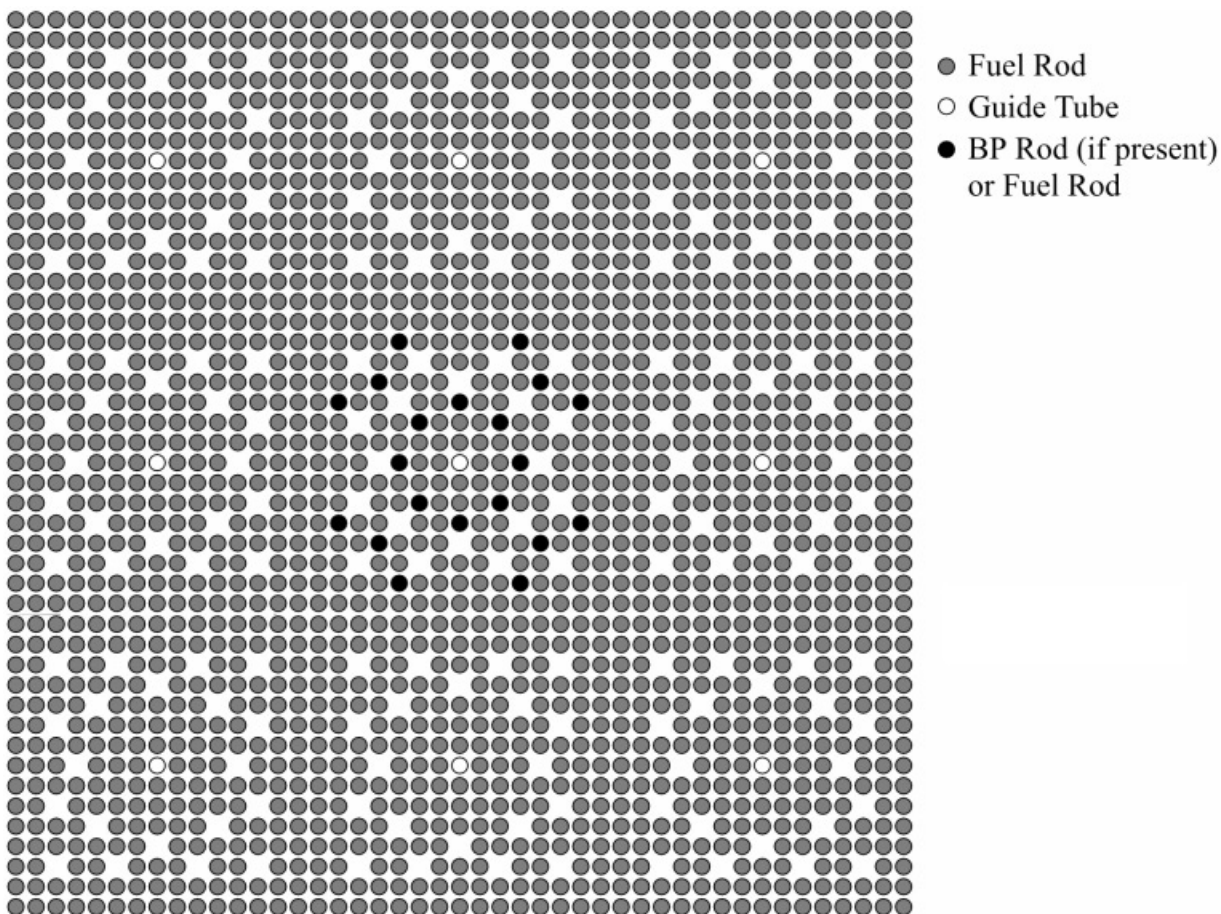


Fig. 6. Square-design experiment lattice.

Because they model water holes in a fuel rod array of a PWR assembly, the 20 empty nonfuel holes are referred to as water holes. Additionally, there is one guide tube at the center of each assembly. For the absorber rod cases, 20 BP rods will replace 20 fuel rods in the center assembly, as shown in Fig. 6. This design requires 1836 fuel rods.

III.D.2. Cruciform Experiment Series

For the cruciform experiment series, the rods will be arranged in a pattern that resembles five 17×17 assemblies in a cruciform pattern. Each of the 17×17 assemblies contains 20 water holes and one central guide tube. In each corner of the cruciform arrangement, there is an 8×8 array of fuel rods. These corner arrays do not contain water holes. For the absorber rod cases, 20 BP rods will replace 20 fuel rods in the center assembly, as shown in Fig. 7. This design requires 1596 fuel rods.

IV. EXISTING EXPERIMENTS

To assess the need for new experimental data, ORNL performed a review of existing critical benchmark ex-

periments with ^{235}U enrichments in the range of 5 to 10 wt%. This review of existing experiments was restricted to configurations listed in the “International Handbook of Evaluated Criticality Safety Benchmark Experiments”⁷ (IHECSBE). For inclusion in this analysis, 123 critical configurations were selected. Summaries of the analyzed compound and solution experiments are provided in Tables V and VI, respectively.

V. TSUNAMI ANALYSIS TECHNIQUES

TSUNAMI techniques from SCALE 5 were used to assess the similarity of the existing and proposed benchmark experiments to the prototypic commercial fuel designs. The TSUNAMI-3D sequence utilizes the KENO V.a Monte Carlo code and computes the sensitivity of k_{eff} to cross-section data on a groupwise and nuclide-reaction-specific basis.⁴ These sensitivity data can be coupled with the uncertainty in the cross-section data to produce an uncertainty in k_{eff} due to uncertainties in the basic nuclear data.³ As cross-section data are believed to be a likely cause of computational biases, a benchmark

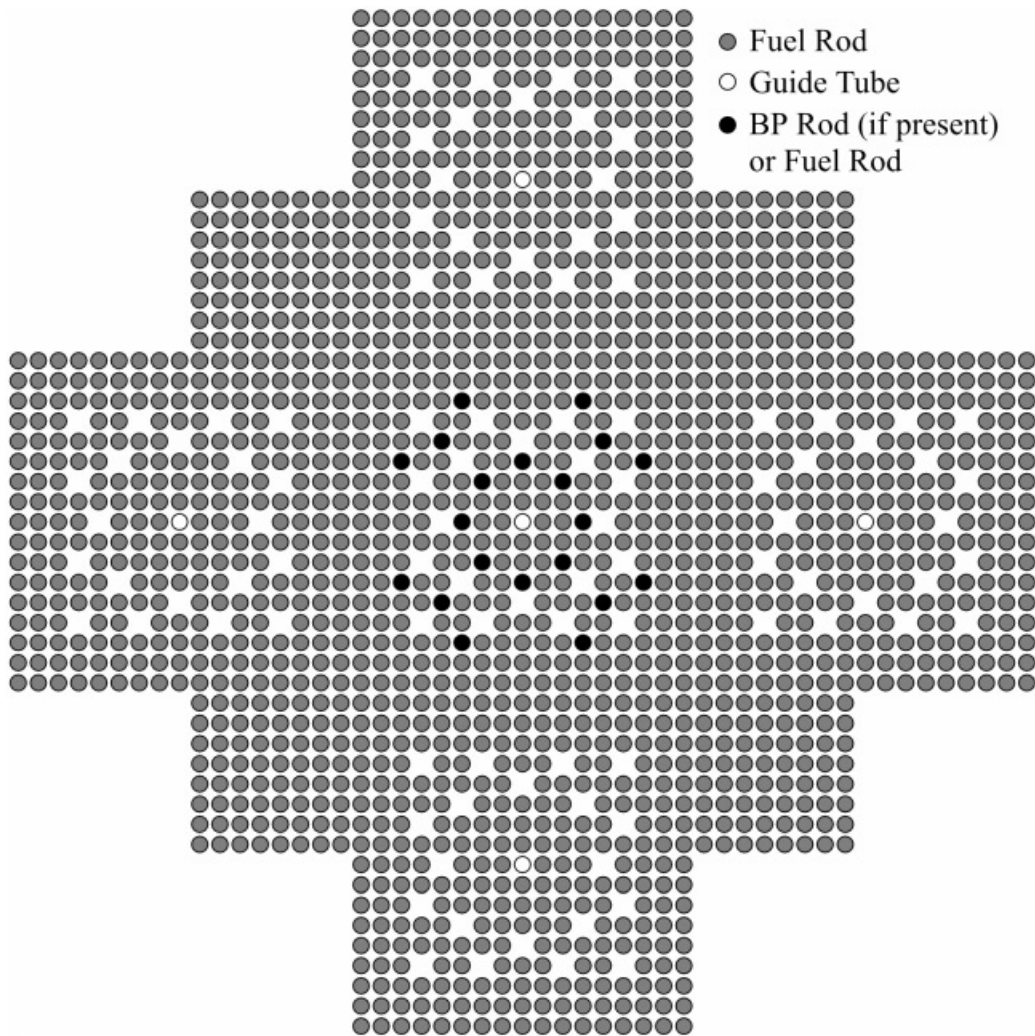


Fig. 7. Cruciform-design experiment lattice.

experiment with uncertainties in k_{eff} that are highly correlated to the uncertainties in the design system will provide a good indication of the expected computational bias. The SCALE 5 code TSUNAMI-IP processes the sensitivity data and cross-section-covariance data and produces a correlation coefficient, denoted c_k , that provides an indication of the similarity of a given benchmark experiment to a design system in terms of the correlations in the uncertainties between the two systems. This correlation coefficient is normalized such that a c_k value of 1.0 indicates that the two systems are identical and a c_k value of 0.0 indicates that the two systems are completely dissimilar. The c_k correlation coefficient is a global integral index in that it produces a single value from information about all nuclides and all reactions of both systems on an energy-dependent basis. Thus, the computed value of c_k provides an indication of the overall similarity of two systems. A brief derivation of global integral index c_k is provided in Appendix A.

TSUNAMI-IP also provides the ability to use sensitivity data to investigate the coverage provided by a benchmark experiment for a certain nuclide-reaction pair. The nuclide-reaction-specific integral index g provides an indication of how well an experiment tests a particular cross-section data component relative to its use in the application.⁸ In the calculation of the g index, the sensitivity of k_{eff} to the cross-section data component for a single energy group of a particular nuclide-reaction pair is examined for a single experiment in relation to a single application. If the experiment's sensitivity for the data component is at least as great as that of the application, then this particular data component is considered covered by the experiment. If the experiment's sensitivity to the data component is not as great as the application's, then only partial coverage is provided. The g index is the fraction of the total sensitivity of the application that is covered by the experiment for the particular nuclide-reaction

TABLE V
Compound Benchmark Critical Experiments Included in TSUNAMI Analysis

Number	Identification	Type	Enrichment (wt%)	Lattice Pitch (cm)
1	IEU-MET-FAST-007-001	Metal alloy	9.9	
2	LEU-COMP-THERM-018-001	Square-pitched array	7.0	1.32
3	LEU-COMP-THERM-019-001	Hexagonally pitched array	5.19	0.7
4	LEU-COMP-THERM-019-002	Hexagonally pitched array	5.19	0.8
5	LEU-COMP-THERM-019-003	Hexagonally pitched array	5.19	1.4
6	LEU-COMP-THERM-020-001	Hexagonally pitched array	5.0	1.3
7	LEU-COMP-THERM-020-002	Hexagonally pitched array	5.0	1.3
8	LEU-COMP-THERM-020-003	Hexagonally pitched array	5.0	1.3
9	LEU-COMP-THERM-020-004	Hexagonally pitched array	5.0	1.3
10	LEU-COMP-THERM-020-005	Hexagonally pitched array	5.0	1.3
11	LEU-COMP-THERM-020-006	Hexagonally pitched array	5.0	1.3
12	LEU-COMP-THERM-020-007	Hexagonally pitched array	5.0	1.3
13	LEU-COMP-THERM-021-001	Hexagonally pitched array + soluble boron	5.0	1.0
14	LEU-COMP-THERM-021-002	Hexagonally pitched array + soluble boron	5.0	1.0
15	LEU-COMP-THERM-021-003	Hexagonally pitched array + soluble boron	5.0	1.0
16	LEU-COMP-THERM-021-004	Hexagonally pitched array + soluble boron	5.0	1.3
17	LEU-COMP-THERM-021-005	Hexagonally pitched array + soluble boron	5.0	1.3
18	LEU-COMP-THERM-021-006	Hexagonally pitched array + soluble boron	5.0	1.3
19	LEU-COMP-THERM-022-001	Hexagonally pitched array	9.83	0.7
20	LEU-COMP-THERM-022-002	Hexagonally pitched array	9.83	0.8
21	LEU-COMP-THERM-022-003	Hexagonally pitched array	9.83	1.0
22	LEU-COMP-THERM-022-004	Hexagonally pitched array	9.83	1.22
23	LEU-COMP-THERM-022-005	Hexagonally pitched array	9.83	1.4
24	LEU-COMP-THERM-022-006	Hexagonally pitched array	9.83	1.83
25	LEU-COMP-THERM-022-007	Hexagonally pitched array	9.83	1.85
26	LEU-COMP-THERM-023-001	Hexagonally pitched array	9.83	1.4
27	LEU-COMP-THERM-023-002	Hexagonally pitched array	9.83	1.4
28	LEU-COMP-THERM-023-003	Hexagonally pitched array	9.83	1.4
29	LEU-COMP-THERM-023-004	Hexagonally pitched array	9.83	1.4
30	LEU-COMP-THERM-023-005	Hexagonally pitched array	9.83	1.4
31	LEU-COMP-THERM-023-006	Hexagonally pitched array	9.83	1.4
32	LEU-COMP-THERM-024-001	Square-pitched array	9.83	0.62
33	LEU-COMP-THERM-024-002	Hexagonally pitched array	9.83	0.88
34	LEU-COMP-THERM-025-001	Hexagonally pitched array	7.41	0.7
35	LEU-COMP-THERM-025-002	Hexagonally pitched array	7.41	0.8
36	LEU-COMP-THERM-025-003	Hexagonally pitched array	7.41	1.0
37	LEU-COMP-THERM-025-004	Hexagonally pitched array	7.41	1.22
38	LEU-COMP-THERM-026-001	Hexagonally pitched array	4.92	1.29
39	LEU-COMP-THERM-026-002	Hexagonally pitched array	4.92	1.29
40	LEU-COMP-THERM-026-003	Hexagonally pitched array	4.92	1.09
41	LEU-COMP-THERM-026-004	Hexagonally pitched array	4.92	1.09
42	LEU-COMP-THERM-032-001	Hexagonally pitched array	9.83	0.7
43	LEU-COMP-THERM-032-002	Hexagonally pitched array	9.83	0.7
44	LEU-COMP-THERM-032-003	Hexagonally pitched array	9.83	0.7
45	LEU-COMP-THERM-032-004	Hexagonally pitched array	9.83	1.4
46	LEU-COMP-THERM-032-005	Hexagonally pitched array	9.83	1.4
47	LEU-COMP-THERM-032-006	Hexagonally pitched array	9.83	1.4
48	LEU-COMP-THERM-032-007	Hexagonally pitched array	9.83	1.85
49	LEU-COMP-THERM-032-008	Hexagonally pitched array	9.83	1.85
50	LEU-COMP-THERM-032-009	Hexagonally pitched array	9.83	1.85

pair, integrated over all energy groups. Where the g index has a value of 1.0, the sensitivity of the k_{eff} of the application for the given nuclide-reaction pair is fully covered by the benchmark experiment across the entire

energy spectrum. Where the g index has a value of 0.0, the benchmark experiment provides no coverage at any energy for the given data. The nuclide-reaction-specific integral index g is discussed further in Appendix B, and

TABLE VI
Solution Benchmark Critical Experiments Included in TSUNAMI Analysis

Number	Identification	Type	Enrichment (wt%)	Uranium Concentration (g/ℓ)
51	LEU-SOL-THERM-001-001	Cylindrical solution tank	4.94	978.3
52	LEU-SOL-THERM-003-001	Spherical solution tank	10.07	296.0
53	LEU-SOL-THERM-003-002	Spherical solution tank	10.07	264.0
54	LEU-SOL-THERM-003-003	Spherical solution tank	10.07	260.0
55	LEU-SOL-THERM-003-004	Spherical solution tank	10.07	255.0
56	LEU-SOL-THERM-003-005	Spherical solution tank	10.07	203.0
57	LEU-SOL-THERM-003-006	Spherical solution tank	10.07	197.0
58	LEU-SOL-THERM-003-007	Spherical solution tank	10.07	193.0
59	LEU-SOL-THERM-003-008	Spherical solution tank	10.07	171.0
60	LEU-SOL-THERM-003-009	Spherical solution tank	10.07	168.0
61	LEU-SOL-THERM-004-001	Cylindrical solution tank	9.97	310.1
62	LEU-SOL-THERM-004-002	Cylindrical solution tank	9.97	290.4
63	LEU-SOL-THERM-004-003	Cylindrical solution tank	9.97	270.0
64	LEU-SOL-THERM-004-004	Cylindrical solution tank	9.97	253.6
65	LEU-SOL-THERM-004-005	Cylindrical solution tank	9.97	241.9
66	LEU-SOL-THERM-004-006	Cylindrical solution tank	9.97	233.2
67	LEU-SOL-THERM-004-007	Cylindrical solution tank	9.97	225.3
68	LEU-SOL-THERM-005-001	Cylindrical solution tank	5.64	400.2
69	LEU-SOL-THERM-005-002	Cylindrical solution tank	5.64	400.2
70	LEU-SOL-THERM-005-003	Cylindrical solution tank	5.64	400.2
71	LEU-SOL-THERM-006-001	Cylindrical solution tank	10.07	420.5
72	LEU-SOL-THERM-006-002	Cylindrical solution tank	10.07	420.5
73	LEU-SOL-THERM-006-003	Cylindrical solution tank	10.07	420.5
74	LEU-SOL-THERM-006-004	Cylindrical solution tank	10.07	420.5
75	LEU-SOL-THERM-006-005	Cylindrical solution tank	10.07	420.5
76	LEU-SOL-THERM-007-001	Cylindrical solution tank	9.97	313.0
77	LEU-SOL-THERM-007-002	Cylindrical solution tank	9.97	290.7
78	LEU-SOL-THERM-007-003	Cylindrical solution tank	9.97	270.0
79	LEU-SOL-THERM-007-004	Cylindrical solution tank	9.97	253.9
80	LEU-SOL-THERM-007-005	Cylindrical solution tank	9.97	241.9
81	LEU-SOL-THERM-008-001	Spherical solution tank	9.97	240.2
82	LEU-SOL-THERM-008-002	Spherical solution tank	9.97	240.7
83	LEU-SOL-THERM-008-003	Spherical solution tank	9.97	241.1
84	LEU-SOL-THERM-008-004	Spherical solution tank	9.97	239.8
85	LEU-SOL-THERM-009-001	Spherical solution tank	9.97	244.7
86	LEU-SOL-THERM-009-002	Spherical solution tank	9.97	245.0
87	LEU-SOL-THERM-009-003	Spherical solution tank	9.97	245.2
88	LEU-SOL-THERM-010-001	Spherical solution tank	9.97	242.1
89	LEU-SOL-THERM-010-002	Spherical solution tank	9.97	242.5
90	LEU-SOL-THERM-010-003	Spherical solution tank	9.97	242.8
91	LEU-SOL-THERM-010-004	Spherical solution tank	9.97	243.3
92	LEU-SOL-THERM-016-001	Slab solution tank	9.97	464.2
93	LEU-SOL-THERM-016-002	Slab solution tank	9.97	429.9
94	LEU-SOL-THERM-016-003	Slab solution tank	9.97	371.9
95	LEU-SOL-THERM-016-004	Slab solution tank	9.97	350.8
96	LEU-SOL-THERM-016-005	Slab solution tank	9.97	328.9
97	LEU-SOL-THERM-016-006	Slab solution tank	9.97	311.4
98	LEU-SOL-THERM-016-007	Slab solution tank	9.97	299.6
99	LEU-SOL-THERM-017-001	Slab solution tank	9.97	464.2
100	LEU-SOL-THERM-017-002	Slab solution tank	9.97	432.4
101	LEU-SOL-THERM-017-003	Slab solution tank	9.97	369.7
102	LEU-SOL-THERM-017-004	Slab solution tank	9.97	350.6
103	LEU-SOL-THERM-017-005	Slab solution tank	9.97	328.9
104	LEU-SOL-THERM-017-006	Slab solution tank	9.97	315.3

(Continued)

TABLE VI (Continued)

Number	Identification	Type	Enrichment (wt%)	Uranium Concentration (g/l)
105	LEU-SOL-THERM-018-001	Slab solution tank	9.97	308.1
106	LEU-SOL-THERM-018-003	Slab solution tank	9.97	312.7
107	LEU-SOL-THERM-018-004	Slab solution tank	9.97	313.2
108	LEU-SOL-THERM-018-005	Slab solution tank	9.97	313.8
109	LEU-SOL-THERM-018-006	Slab solution tank	9.97	314.6
110	LEU-SOL-THERM-019-001	Slab solution tank	9.97	317.1
111	LEU-SOL-THERM-019-002	Slab solution tank	9.97	315.8
112	LEU-SOL-THERM-019-003	Slab solution tank	9.97	316.3
113	LEU-SOL-THERM-019-004	Slab solution tank	9.97	317.1
114	LEU-SOL-THERM-019-005	Slab solution tank	9.97	317.7
115	LEU-SOL-THERM-019-006	Slab solution tank	9.97	318.4
116	LEU-SOL-THERM-020-001	Cylindrical solution tank	9.97	243.1
117	LEU-SOL-THERM-020-002	Cylindrical solution tank	9.97	225.5
118	LEU-SOL-THERM-020-003	Cylindrical solution tank	9.97	204.7
119	LEU-SOL-THERM-020-004	Cylindrical solution tank	9.97	193.7
120	LEU-SOL-THERM-021-001	Cylindrical solution tank	9.97	243.1
121	LEU-SOL-THERM-021-002	Cylindrical solution tank	9.97	225.7
122	LEU-SOL-THERM-021-003	Cylindrical solution tank	9.97	204.7
123	LEU-SOL-THERM-021-004	Cylindrical solution tank	9.97	193.7

all of the TSUNAMI techniques are explained in greater detail in the SCALE 5 manual.⁵

The TSUNAMI-3D analysis sequence was used to generate sensitivity data for each prototypic commercial fuel design described in Sec. II, each proposed experiment described in Sec. III, and each existing experiment described in Sec. IV. The SCALE 238-group ENDF/B-V library was used in each analysis.

The global integral index c_k was computed for each commercial design in relation to each experiment. The c_k index relies on the existence of cross-section-covariance data, but several nuclide-reaction pairs in ENDF/B-V do not have covariance data. For these nuclide-reaction pairs, an uncertainty value of 5% standard deviation was used in TSUNAMI-IP. Important nuclide-reaction pairs for which the 5% uncertainty data were used are all nuclides and reactions of Gd and Zr and the ^{238}U fission energy distribution χ . The nuclide-reaction-specific integral index g was also computed for each experiment in relation to each commercial design.

Current guidance³ states that an experiment is adequately similar to a design application to serve in its code validation if the c_k value relating the experiment to the application is 0.9 or higher. The experiment may be applicable to the code validation if its c_k value is 0.8 or higher. Furthermore, to ensure that the correct computational bias is determined for a given application, approximately 15 to 20 experiments with c_k values of at least 0.9 or 25 to 40 experiments with c_k values between 0.8 and 0.9 are recommended. Although not fully investigated, it is expected that fewer experiments with c_k values near

1.0 should also provide for an adequate assessment of the computational bias.

VI. APPLICABILITY OF EXISTING EXPERIMENTS

The similarity of the 123 existing experiments to the prototypic commercial fuel designs was assessed using the integral index c_k generated from the TSUNAMI-IP code. The results of this analysis are depicted in Figs. 8 through 11 for the low-temperature B&W, high-temperature B&W, Westinghouse, and GE commercial fuel designs, respectively. The experiment numbers given on the x axis correspond to the numbers listed in Tables V and VI. The integral index values given on the y axis correspond to the value of c_k for the particular commercial fuel design in relation to the particular experiment.

The numbers of experiments with c_k values exceeding 0.9 for each application are given in Table VII. The maximum number of experiments with c_k values of at least 0.9 for any application is 7 and occurs for B&W 7 and 10% enriched low-temperature assemblies with no BPs, Westinghouse 10% enriched low- and high-temperature assemblies with no BPs, and the GE 10% enriched high-temperature assembly. Four applications, the GE 4, 6, 7, and 10% enriched low-temperature assemblies with eight BPs, had no experiments with c_k values exceeding 0.9.

The numbers of experiments with c_k values exceeding 0.8 are given in Table VIII. The number of

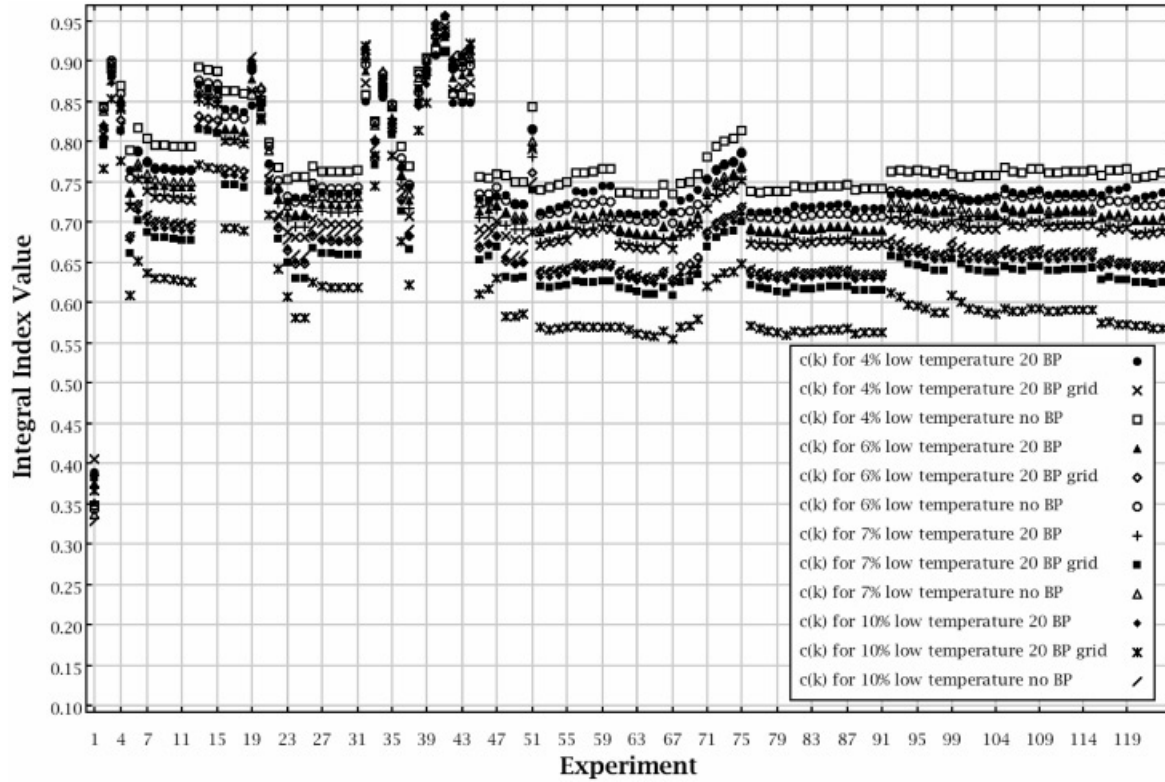


Fig. 8. Values of integral index c_k for 123 existing experiments with low-temperature B&W assemblies.

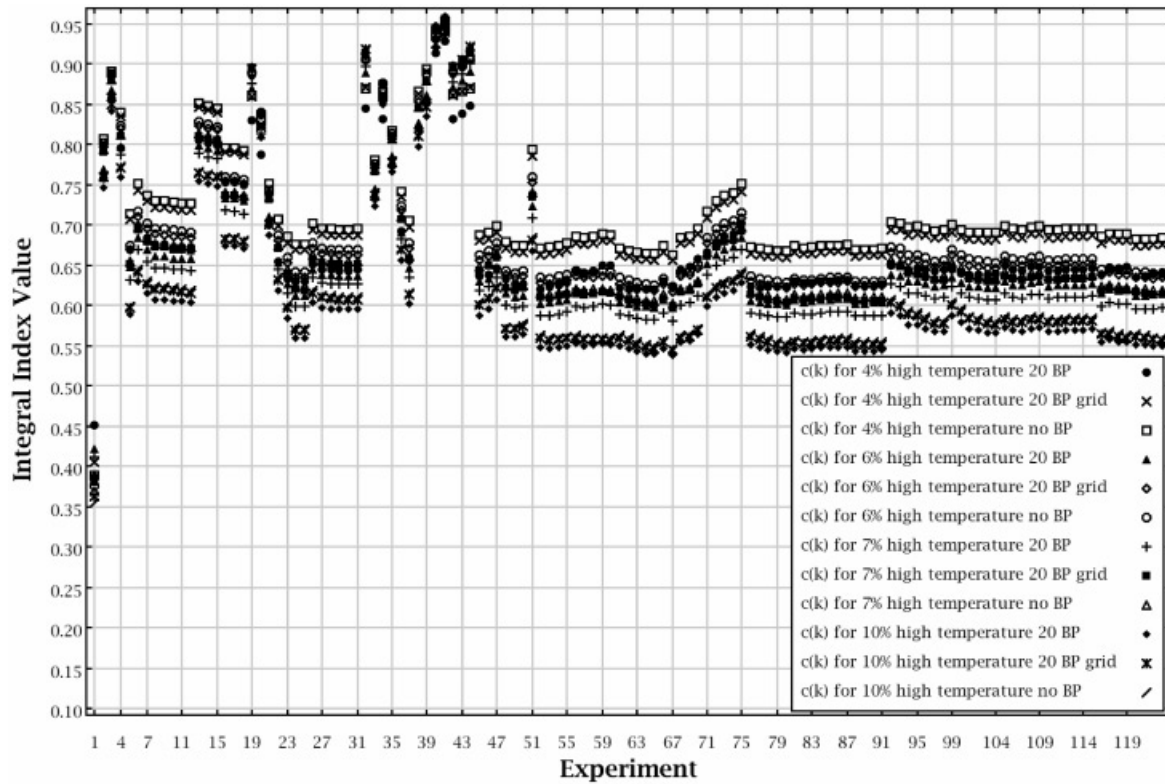


Fig. 9. Values of integral index c_k for 123 existing experiments with high-temperature B&W assemblies.

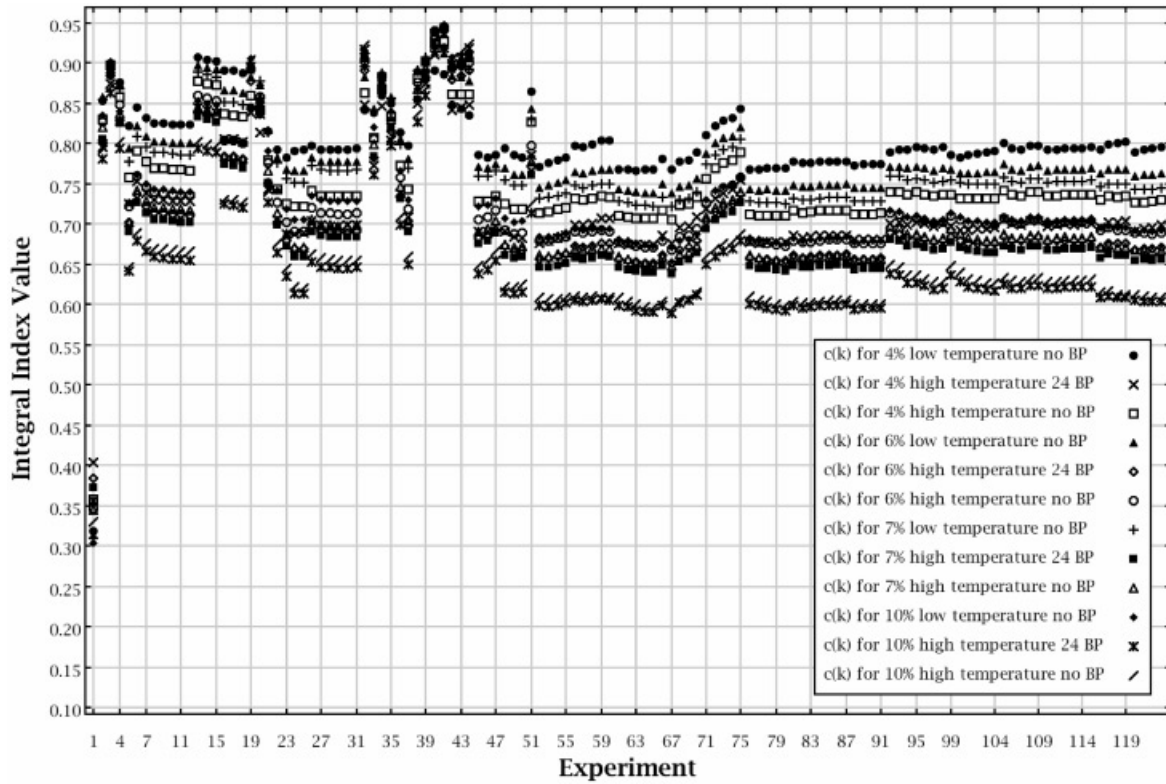


Fig. 10. Values of integral index c_k for 123 existing experiments with Westinghouse assemblies.

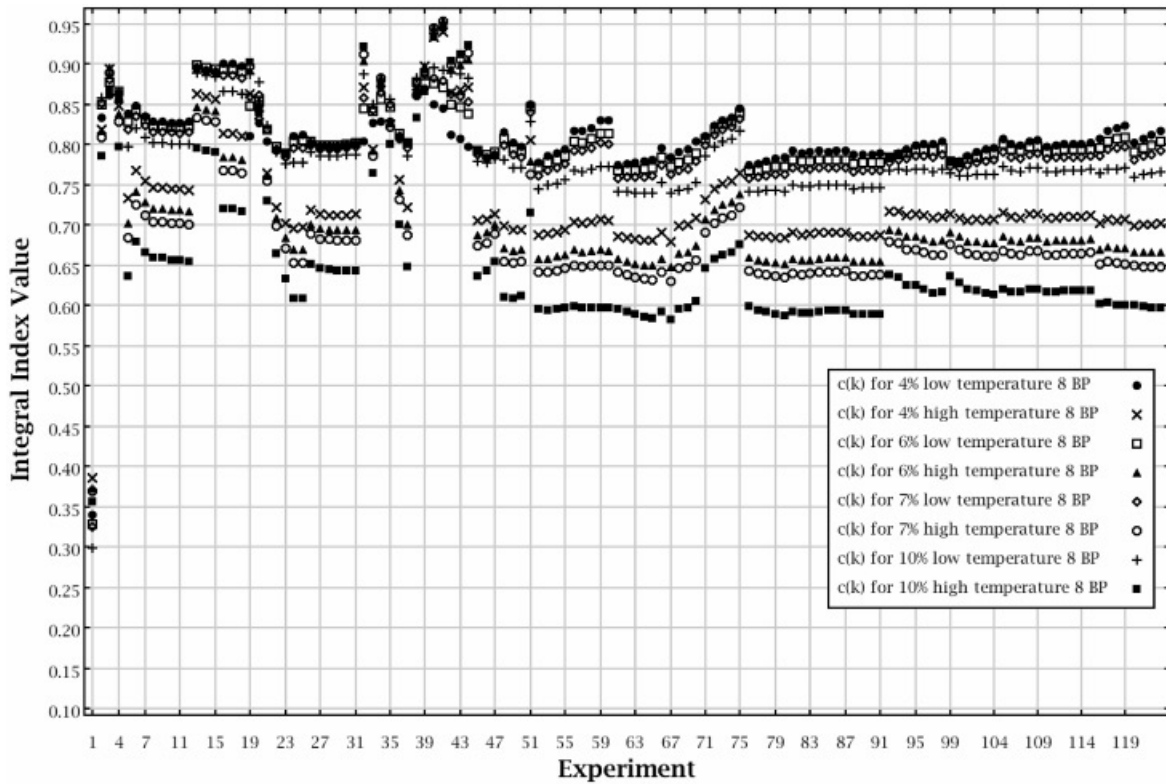


Fig. 11. Values of integral index c_k for 123 existing experiments with GE assemblies.

TABLE VII
Numbers of Existing Experiments with c_k Values ≥ 0.9 for Prototypic Commercial Fuel Designs

Enrichment (%)	Assembly	Low Temperature			High Temperature		
		All BP	BP Grid	No BP	All BP	BP Grid	No BP
4	B&W 15 × 15	2	2	3	2	2	2
	Westinghouse 17 × 17			3	2		3
	GE 8 × 8	0			2		
6	B&W 15 × 15	2	5	3	2	4	4
	Westinghouse 17 × 17			4	2		5
	GE 8 × 8	0			4		
7	B&W 15 × 15	2	5	7	3	5	5
	Westinghouse 17 × 17			4	4		6
	GE 8 × 8	0			5		
10	B&W 15 × 15	6	5	7	4	5	5
	Westinghouse 17 × 17			7	5		7
	GE 8 × 8	0			7		

TABLE VIII
Numbers of Existing Experiments with c_k Values ≥ 0.8 for Prototypic Commercial Fuel Designs

Enrichment (%)	Assembly	Low Temperature			High Temperature		
		All BP	BP Grid	No BP	All BP	BP Grid	No BP
4	B&W 15 × 15	23	20	28	13	18	18
	Westinghouse 17 × 17			42	20		23
	GE 8 × 8	68			22		
6	B&W 15 × 15	22	18	23	12	17	18
	Westinghouse 17 × 17			36	18		22
	GE 8 × 8	54			18		
7	B&W 15 × 15	21	17	23	12	17	17
	Westinghouse 17 × 17			26	18		18
	GE 8 × 8	39			18		
10	B&W 15 × 15	18	12	18	11	12	12
	Westinghouse 17 × 17			22	12		15
	GE 8 × 8	35			13		

experiments with c_k values exceeding 0.8, including those exceeding 0.9, ranges from a minimum of 11 for the B&W 10% enriched high-temperature assembly with 20 BPs to a maximum 68 for the GE 4% enriched low-temperature assembly with 8 BPs.

Although the TSUNAMI techniques identify a number of existing experiments as applicable to the prototypic commercial fuel designs, these experiments are not suitable for modeling with U.S. commercial reactor physics codes. The vast majority of experiments with c_k val-

ues exceeding 0.9 are hexagonally pitched arrays of fuel rods. Many commercial reactor physics codes model only square-pitched arrays. The hexagonally pitched arrays are suitable for modeling in Monte Carlo codes commonly used for criticality safety analyses. For the two square-pitched-array lattice configurations, experiment 2 is not fully flooded, and the rods are arranged in a circular pattern. Experiment 32, although fully flooded, contains one row with a different number of fuel rods from the remainder of the critical lattice. Neither of these

experiments could be suitably modeled in many commercial reactor physics codes. TSUNAMI also revealed that some solution systems produced c_k values in excess of 0.8, especially for the low-temperature GE configurations. These results reveal that although the geometrical configurations of these systems are quite different, they are utilizing the cross-section data in a similar manner.

VII. APPLICABILITY OF PROPOSED EXPERIMENTS

The similarity of the 16 proposed experiments to the prototypic commercial fuel designs was assessed using the integral index c_k generated from the TSUNAMI-IP code. The results of this analysis are depicted in Figs. 12 through 15 for the B&W cold, B&W hot, Westinghouse, and GE commercial fuel designs, respectively. The experiment numbers given on the x axis correspond to the numbers listed in Table IX. The integral index values given on the y axis correspond to the value of c_k for the particular commercial fuel design in relation to the particular experiment.

As shown in Figs. 12 through 15 and summarized in Table X, all proposed experiments have c_k values ≥ 0.8 in relation to all studied prototypic commercial fuel design

applications. Several experimental configurations have c_k values ≥ 0.9 in relation to some particular applications, demonstrating highly correlated uncertainties and good applicability for code validation studies.

The numbers of experiments with c_k values ≥ 0.9 for each application are given in Table XI. None of the proposed experiments produce a c_k value of at least 0.9 for 4% enriched fuel. Several experiments produce c_k values ≥ 0.9 for 6, 7, and 10% enriched low-temperature B&W and Westinghouse assemblies with no BPs. Nine of the experiments produce a $c_k \geq 0.9$ for the GE 10% enriched low-temperature assembly with eight BPs, and seven of the experiments produce a $c_k \geq 0.9$ for the 6% enriched Westinghouse high-temperature assembly with no BPs.

The numbers of experiments with c_k values ≥ 0.9 are detailed by experiment type, square and cruciform, in Tables XII and XIII, respectively. As seen in Tables XII and XIII, all eight square-design experiments have c_k values ≥ 0.9 for the 7% enriched low-temperature B&W and Westinghouse assemblies with no BPs. A minimum of six square configurations have c_k values ≥ 0.9 for the 6% enriched low-temperature B&W and Westinghouse assemblies with no BPs. Six configurations have c_k values ≥ 0.9 for the 10% enriched low-temperature Westinghouse assembly with no BPs, and five configurations

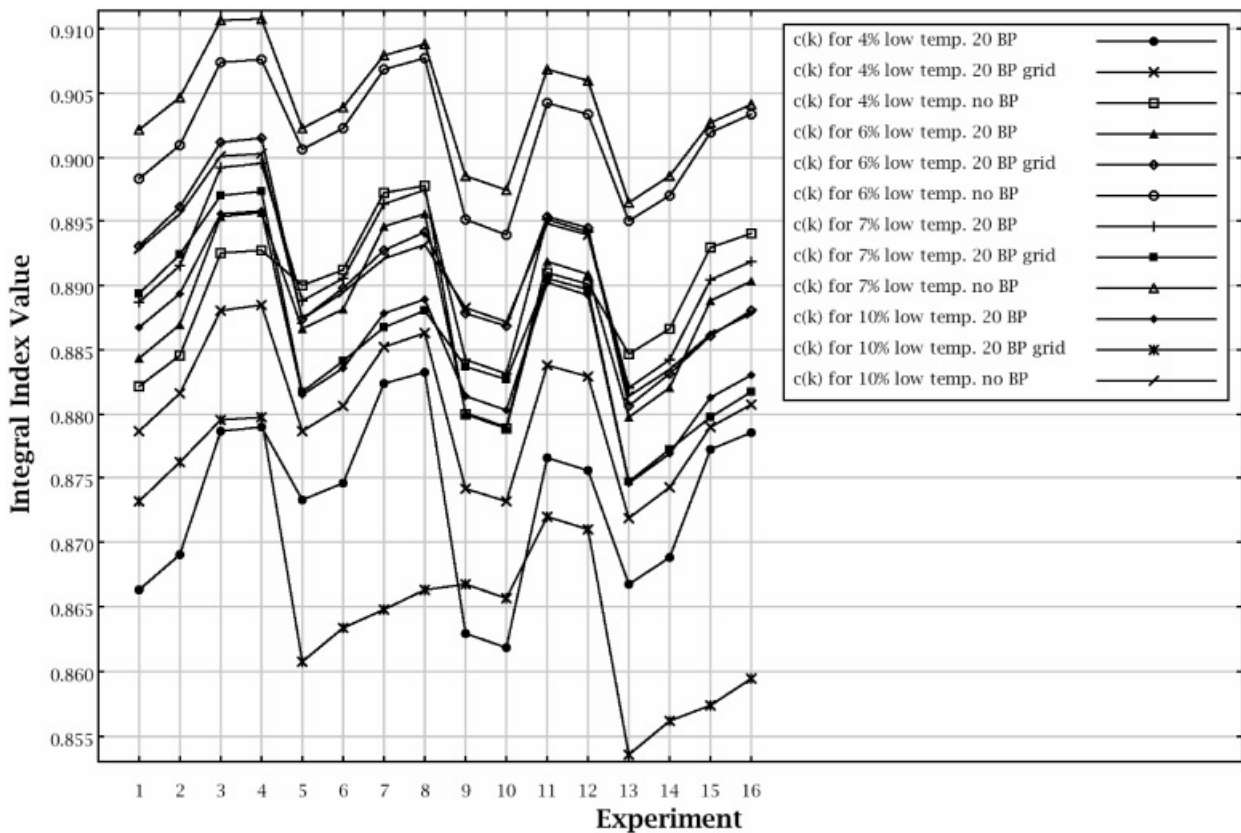


Fig. 12. Values of integral index c_k for 16 proposed experiments with low-temperature B&W assemblies.

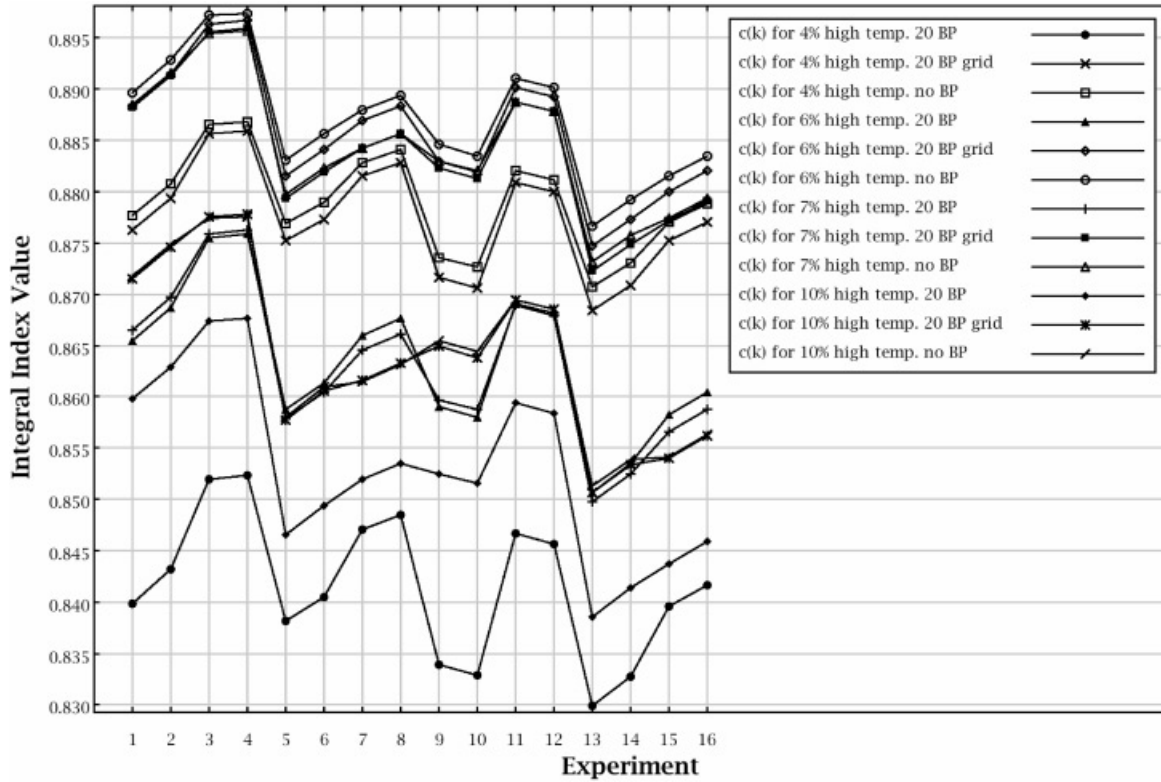


Fig. 13. Values of integral index c_k for 16 proposed experiments with high-temperature B&W assemblies.

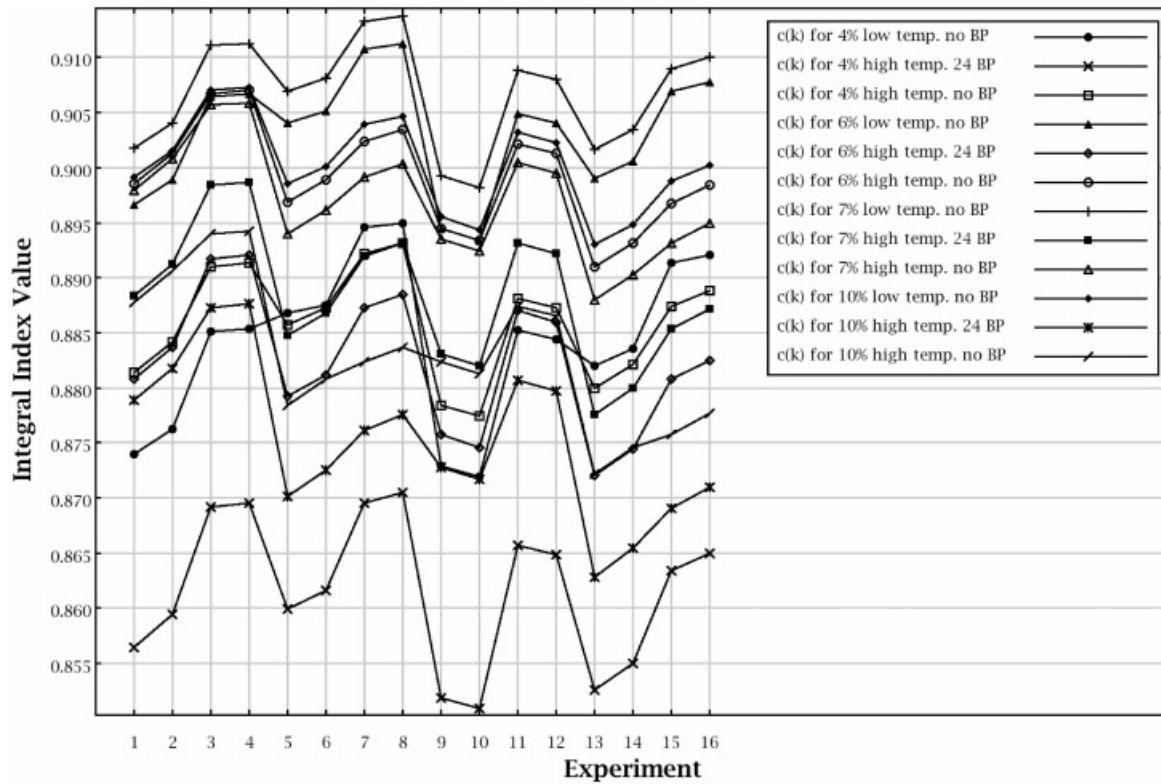


Fig. 14. Values of integral index c_k for 16 proposed experiments with Westinghouse assemblies.

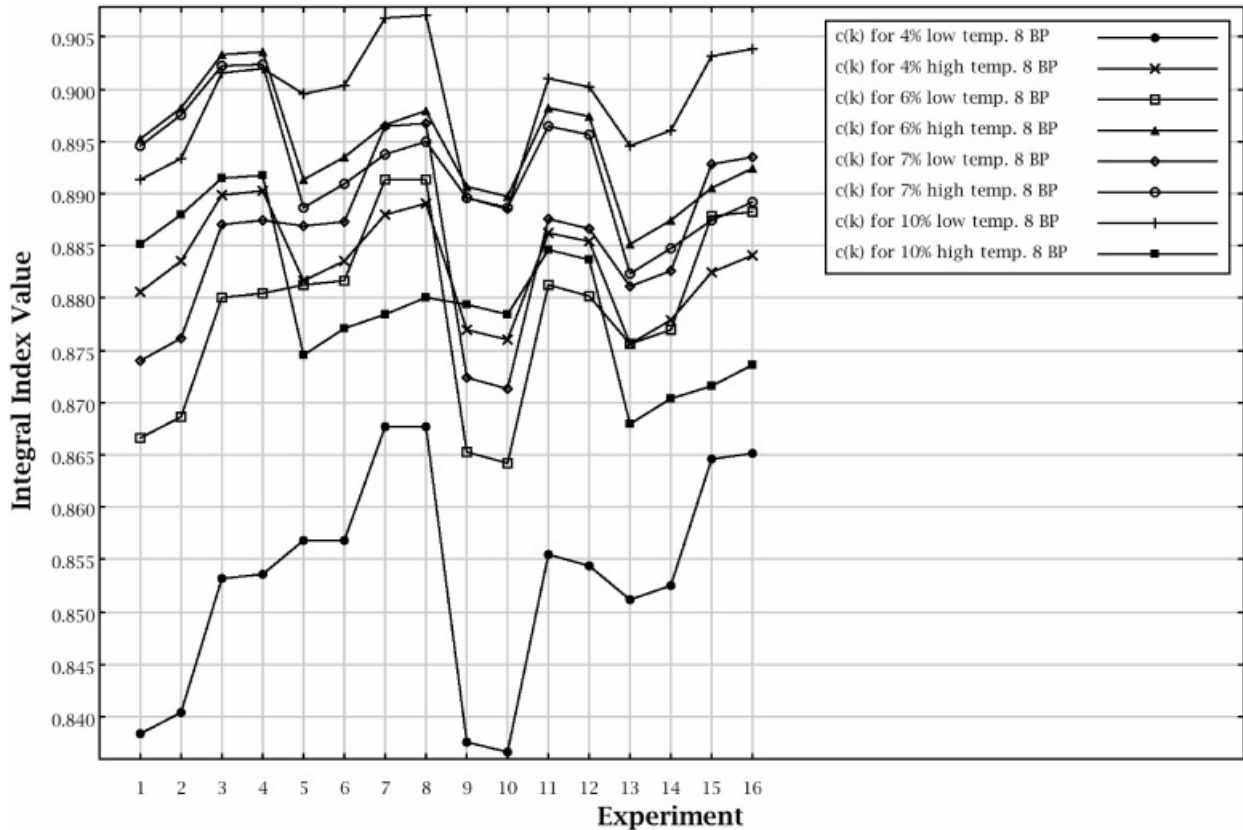


Fig. 15. Values of integral index c_k for 16 proposed experiments with GE assemblies.

have c_k values ≥ 0.9 for the 6% enriched high-temperature Westinghouse assembly with no BPs and the 10% enriched low-temperature GE assembly with eight BPs.

For the cruciform experiments, a maximum of six have c_k values ≥ 0.9 for the 7% enriched low-temperature Westinghouse assembly with no BPs, five have c_k values ≥ 0.9 for the 6% enriched low-temperature Westinghouse assembly with no BPs, and four have c_k values ≥ 0.9 for the 6 and 7% enriched low-temperature B&W assemblies with no BPs and 10% enriched low-temperature GE assembly with eight BPs.

Based on this analysis, all of the proposed experiments provide useful validation data for the selected prototypic commercial fuel designs, as each experiment produces c_k values ≥ 0.8 for numerous commercial assemblies. Furthermore, the square-design experiments provide more useful data than the cruciform-design experiments for these particular applications because more square- than cruciform-design experiments produce c_k values ≥ 0.9 with several commercial assemblies.

VIII. NUCLIDE-REACTION-SPECIFIC ANALYSIS

A nuclide-reaction-specific analysis was performed to examine the coverage provided by the proposed ex-

periments for the prototypic commercial fuel designs using the integral index g . As a demonstration of this technique, only the coverage provided by experiment 4, the square-design experiment with a pitch of 0.8 cm at 60°C with 20 BPs, for the 7% enriched low-temperature assemblies is presented here.

For the 7% enriched low-temperature B&W assembly with 20 BPs, experiment 4 produces a c_k value of 0.89, the highest of any proposed experiment. The nuclide-reaction-specific analysis was used to assess which reactions were well covered and which were not as well covered in the B&W assembly by this particular experiment. Sensitivity profiles for ^{235}U fission and ^{157}Gd capture for this assembly and experiment are shown in Figs. 16 and 17. In Fig. 16, it can be seen that k_{eff} is most sensitive to the ^{235}U fission cross section in the thermal region. The sensitivity of the assembly is slightly greater than that of the experiment, and the experiment does not provide complete coverage for ^{235}U fission for this case.

The integral index g quantifies the sensitivity of the application covered by the experiment. The values of the index g for fission, capture, and scatter for each nuclide in this application in relation to experiment 4 are given in Table XIV. The energy-integrated sensitivity coefficients for the application are also shown in Table XIV. The energy-integrated sensitivity coefficient is the sum

TABLE IX
Proposed Experiments Analyzed with TSUNAMI

Experiment Number	Fuel Arrangement	Pitch (cm)	Absorber	T_{mod} (°C)
1	Square	0.800	None	20
2			None	60
3		0.800	20 Gd rods in center assembly	20
4			20 Gd rods in center assembly	60
5		0.855	None	20
6			None	60
7		0.855	20 Gd rods in center assembly	20
8			20 Gd rods in center assembly	60
9	Cruciform	0.800	None	20
10			None	60
11		0.800	20 Gd rods in center assembly	20
12			20 Gd rods in center assembly	60
13		0.855	None	20
14			None	60
15		0.855	20 Gd rods in center assembly	20
16			20 Gd rods in center assembly	60

of the sensitivity coefficients by group for a particular nuclide-reaction pair. It is equivalent to the area under the sensitivity profile shown in Fig. 16. The nuclide-reaction pair with the highest sensitivity coefficient is ²³⁵U fission with a sensitivity of 0.302. An interpretation of this value is that if the evaluated fission cross section were uniformly increased by 1% across all energies, the computed value of k_{eff} would increase by 0.302%. The value of the g integral index for ²³⁵U fission is 0.94, indicating that the experiment tests the ²³⁵U fission cross section with 94% of its importance to k_{eff} relative to its use in the application.

Also shown in Table XIV, the energy-integrated sensitivity of k_{eff} of the application to ¹⁵⁷Gd capture is -0.0152. For this application, experiment 4 produces a g value of only 0.31 for ¹⁵⁷Gd capture, indicating that only 31% of the application's sensitivity is covered by the experiment. Recall that the proposed experimental configurations only have BPs in the central assembly location. Also, the use of Al cladding in the experiments prevents any validation of the Zr cladding used in the application.

For the 7% enriched low-temperature B&W BP grid configuration, experiment 4 produces a c_k value of 0.89, the highest of any proposed experiment. The sensitivity profile for ¹⁵⁷Gd for this application is shown in Fig. 17. Because ¹⁵⁷Gd capture produces a negative contribution to k_{eff} , the lower the value is, the greater its impact on k_{eff} is. Because only one-third of the assemblies in this model contain 20 BPs, the sensitivity of k_{eff} to the ¹⁵⁷Gd capture

TABLE X
Numbers of 16 Proposed Experiments with c_k Values ≥ 0.8 for Prototypic Commercial Fuel Designs

Enrichment (%)	Assembly	Low Temperature			High Temperature		
		All BP	BP Grid	No BP	All BP	BP Grid	No BP
4	B&W 15 × 15	16	16	16	16	16	16
	Westinghouse 17 × 17			16	16		16
	GE 8 × 8	16			16		
6	B&W 15 × 15	16	16	16	16	16	16
	Westinghouse 17 × 17			16	16		16
	GE 8 × 8	16			16		
7	B&W 15 × 15	16	16	16	16	16	16
	Westinghouse 17 × 17			16	16		16
	GE 8 × 8	16			16		
10	B&W 15 × 15	16	16	16	16	16	16
	Westinghouse 17 × 17			16	16		16
	GE 8 × 8	16			16		

TABLE XI

Numbers of 16 Proposed Experiments with c_k Values ≥ 0.9 for Prototypic Commercial Fuel Designs

Enrichment (%)	Assembly	Low Temperature			High Temperature		
		All BP	BP Grid	No BP	All BP	BP Grid	No BP
4	B&W 15 × 15	0	0	0	0	0	0
	Westinghouse 17 × 17			0	0		0
	GE 8 × 8	0			0		
6	B&W 15 × 15	0	2	11	0	0	0
	Westinghouse 17 × 17			11	0		7
	GE 8 × 8	0			2		
7	B&W 15 × 15	0	0	12	0	0	0
	Westinghouse 17 × 17			14	0		5
	GE 8 × 8	0			2		
10	B&W 15 × 15	0	0	2	0	0	0
	Westinghouse 17 × 17			9	0		0
	GE 8 × 8	9			0		

TABLE XII

Numbers of Eight Proposed Square Experiments with c_k Values ≥ 0.9 for Prototypic Commercial Fuel Designs

Enrichment (%)	Assembly	Low Temperature			High Temperature		
		All BP	BP Grid	No BP	All BP	BP Grid	No BP
4	B&W 15 × 15	0	0	0	0	0	0
	Westinghouse 17 × 17			0	0		0
	GE 8 × 8	0			0		
6	B&W 15 × 15	0	2	7	0	0	0
	Westinghouse 17 × 17			6	0		5
	GE 8 × 8	0			2		
7	B&W 15 × 15	0	0	8	0	0	0
	Westinghouse 17 × 17			8	0		4
	GE 8 × 8	0			2		
10	B&W 15 × 15	0	0	2	0	0	0
	Westinghouse 17 × 17			6	0		0
	GE 8 × 8	5			0		

cross section is reduced relative to the all-BP assembly. For the BP grid configuration, the energy-integrated sensitivity coefficients and values of the g integral index in relation to experiment 4 are shown in Table XV. Here, the sensitivity coefficient for ^{157}Gd capture is -0.00369 , and the g value is 0.91. Thus, experiment 4 provides coverage for 91% of the sensitivity of k_{eff} to ^{157}Gd capture for this application. Experiment 4 also produces a g value of 0.96 for ^{235}U fission, which is slightly improved from the g value of this experiment in relation to the all-BP configuration of

this assembly type, 0.94. Note the presence of ^{10}B and ^{11}B in Table XV due to the 500 ppm boron concentration in the BP grid configurations.

For the 7% enriched low-temperature B&W assembly with no BPs, experiment 4 produces a c_k value of 0.91, the highest of any proposed experiment. The sensitivity profile for ^{235}U for this application is shown in Fig. 16. Here, the magnitude of the sensitivity in the thermal region is reduced relative to the all-BP assembly. The energy-integrated sensitivity coefficients for this assembly and values of the g integral index in relation to

TABLE XIII

Numbers of Eight Proposed Cruciform Experiments with c_k Values ≥ 0.9 for Prototypic Commercial Fuel Designs

Enrichment (%)	Assembly	Low Temperature			High Temperature		
		All BP	BP Grid	No BP	All BP	BP Grid	No BP
4	B&W 15 × 15	0	0	0	0	0	0
	Westinghouse 17 × 17			0	0		0
	GE 8 × 8	0			0		
6	B&W 15 × 15	0	0	4	0	0	0
	Westinghouse 17 × 17			5	0		2
	GE 8 × 8	0			0		
7	B&W 15 × 15	0	0	4	0	0	0
	Westinghouse 17 × 17			6	0		1
	GE 8 × 8	0			0		
10	B&W 15 × 15	0	0	0	0	0	0
	Westinghouse 17 × 17			3	0		0
	GE 8 × 8	4			0		

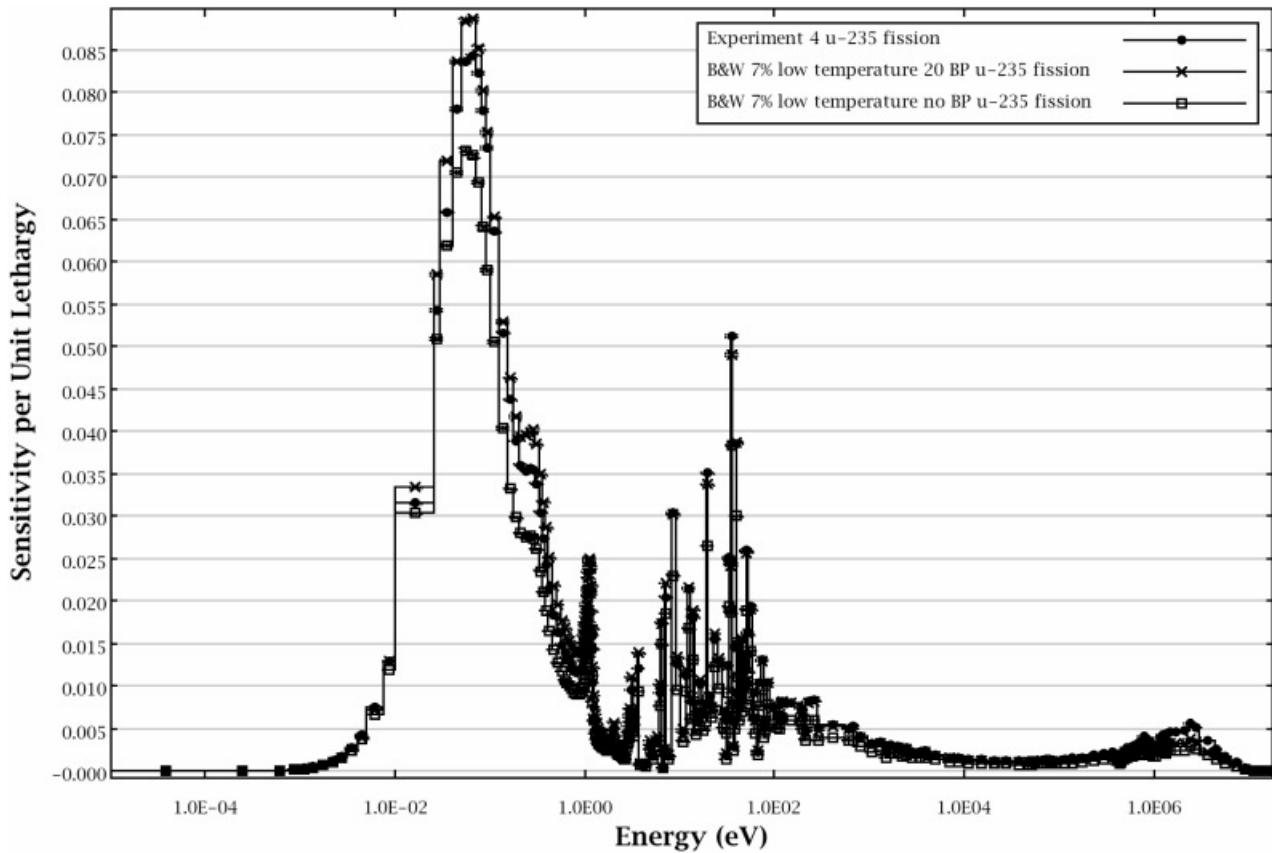


Fig. 16. Sensitivity of k_{eff} to the ^{235}U fission cross section for proposed experiment 4 and 7% enriched low-temperature B&W assemblies with 20 BPs and no BPs.

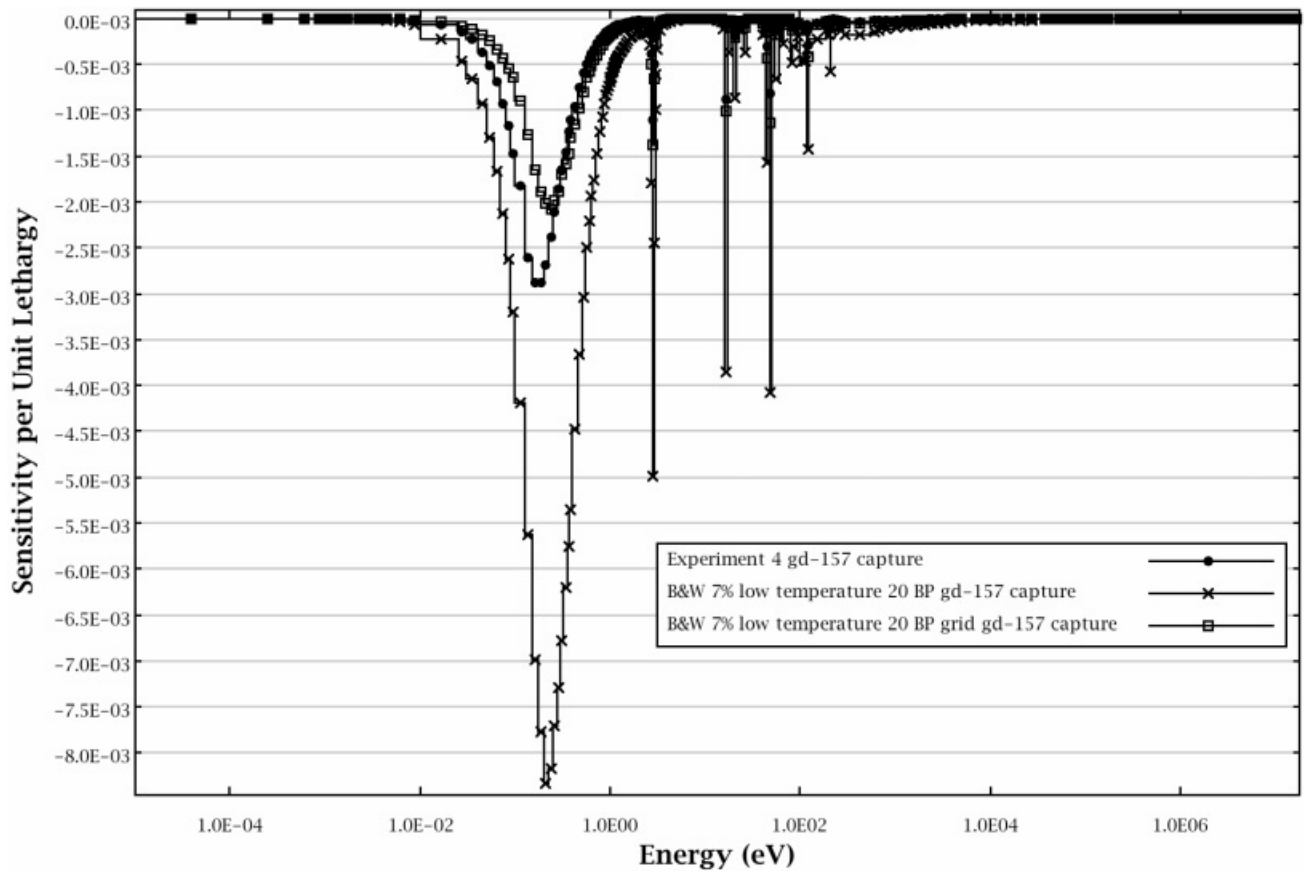


Fig. 17. Sensitivity of k_{eff} to the ^{157}Gd capture cross section for proposed experiment 4 and 7% enriched low-temperature B&W assemblies with 20 BPs and assembly grid configuration where one-third of the assemblies have BPs.

TABLE XIV
Nuclide-Reaction-Specific Analysis of Coverage Provided by Experiment 4 for 7% Enriched Low-Temperature B&W Assembly with 20 BPs

	Fission		Capture		Scatter	
	Sensitivity	g	Sensitivity	g	Sensitivity	g
^1H			$-4.40\text{E}-02^a$	1.0	$9.91\text{E}-02$	0.76
^{16}O			$-4.56\text{E}-03$	0.61	$-4.33\text{E}-03$	0.65
Zr			$-5.09\text{E}-03$	0.0	$-1.04\text{E}-03$	0.0
^{154}Gd			$-1.44\text{E}-04$	0.20	$6.06\text{E}-07$	0.16
^{155}Gd			$-7.70\text{E}-03$	0.25	$5.64\text{E}-06$	0.16
^{156}Gd			$-4.76\text{E}-04$	0.21	$3.38\text{E}-05$	0.17
^{157}Gd			$-1.52\text{E}-02$	0.31	$1.77\text{E}-05$	0.18
^{158}Gd			$-2.55\text{E}-04$	0.21	$3.83\text{E}-06$	0.15
^{160}Gd			$-6.41\text{E}-05$	0.19	$-2.39\text{E}-06$	0.13
^{235}U	$3.02\text{E}-01$	0.9443	$-1.42\text{E}-01$	0.98	$4.55\text{E}-05$	0.56
^{238}U	$2.48\text{E}-02$	1.0000	$-1.38\text{E}-01$	0.97	$8.74\text{E}-03$	0.76

^aRead as -4.40×10^{-2} .

TABLE XV
Nuclide-Reaction-Specific Analysis of Coverage Provided by Experiment 4 for 7% Enriched Low-Temperature B&W Configuration with 20 BPs in One-Third of Assemblies

	Fission		Capture		Scatter	
	Sensitivity	<i>g</i>	Sensitivity	<i>g</i>	Sensitivity	<i>g</i>
¹ H			-3.21E-02 ^a	1.0	1.31E-01	0.85
¹⁶ O			-4.61E-03	0.60	-6.15E-03	0.59
Zr			-5.88E-03	0.0	-1.09E-03	0.0
¹⁵⁴ Gd			-3.95E-05	0.72	3.00E-07	0.43
¹⁵⁵ Gd			-2.00E-03	0.83	2.33E-06	0.38
¹⁵⁶ Gd			-1.31E-04	0.76	1.05E-05	0.54
¹⁵⁷ Gd			-3.69E-03	0.91	6.59E-06	0.49
¹⁵⁸ Gd			-6.96E-05	0.76	1.45E-06	0.40
¹⁶⁰ Gd			-1.80E-05	0.68	-1.26E-07	0.30
²³⁵ U	2.72E-01	0.96	-1.54E-01	0.89	-7.92E-05	0.50
²³⁸ U	2.71E-02	1.0	-1.62E-01	0.85	8.87E-03	0.76
¹⁰ B			-3.23E-02	0.91	-1.73E-08	0.47
¹¹ B			-2.27E-07	0.83	1.64E-07	0.40

^aRead as -3.21 × 10⁻².

experiment 4 are shown in Table XVI. The value of the *g* integral index for ²³⁵U fission is 1.0, demonstrating that all of the sensitivity of ²³⁵U fission in the application is covered by the experiment. Even though the most important nuclide-reaction pair in the application is fully covered by this experiment, the *c_k* value relating to overall system similarity is only 0.91. A reason that *c_k* is not also 1.0 is revealed by comparing the ¹H scatter sensitivity profiles for this assembly and for the experiment, as shown in Fig. 18. At fission neutron energies, the sensitivity for the application is negative, where the sensitivity for the experiment is positive. In the infinite lattice of the application, additional scattering at fission neutron energies reduces the number of neutrons available for fast fission in ²³⁸U and has a negative effect on *k_{eff}*. The sensitivity

of *k_{eff}* to the ²³⁸U fission cross section is also shown in Fig. 18. Note that the ¹H scatter and ²³⁸U capture sensitivities at fission neutron energies are nearly mirror images of each other. With the small size of the experimental core, the negative effect of loss of ²³⁸U fast fission is outweighed by the return of neutrons from ¹H scattering in the reflector. Thus, the sensitivity of *k_{eff}* to ¹H scatter for the experiment is positive at fast energies. This difference in leakage effects propagates to the *c_k* value and reduces the applicability of the experiment to infinite lattice designs.

For the 7% enriched low-temperature Westinghouse assembly with no BPs, experiment 4 produces a *c_k* value of 0.91. The energy-integrated sensitivity coefficients for this assembly and values of the *g* integral index in relation to

TABLE XVI
Nuclide-Reaction-Specific Analysis of Coverage Provided by Experiment 4 for 7% Enriched Low-Temperature B&W Assembly with No BPs

	Fission		Capture		Scatter	
	Sensitivity	<i>g</i>	Sensitivity	<i>g</i>	Sensitivity	<i>g</i>
¹ H			4.86E-02 ^a	1.0	1.22E-01	0.88
¹⁶ O			-4.49E-03	0.62	-3.13E-03	0.69
Zr			-5.32E-03	0.0	-4.87E-04	0.0
²³⁵ U	2.38E-01	1.0	-1.56E-01	0.92	1.84E-04	0.64
²³⁸ U	1.89E-02	1.0	-1.44E-01	0.95	1.02E-02	0.82

^aRead as 4.86 × 10⁻².

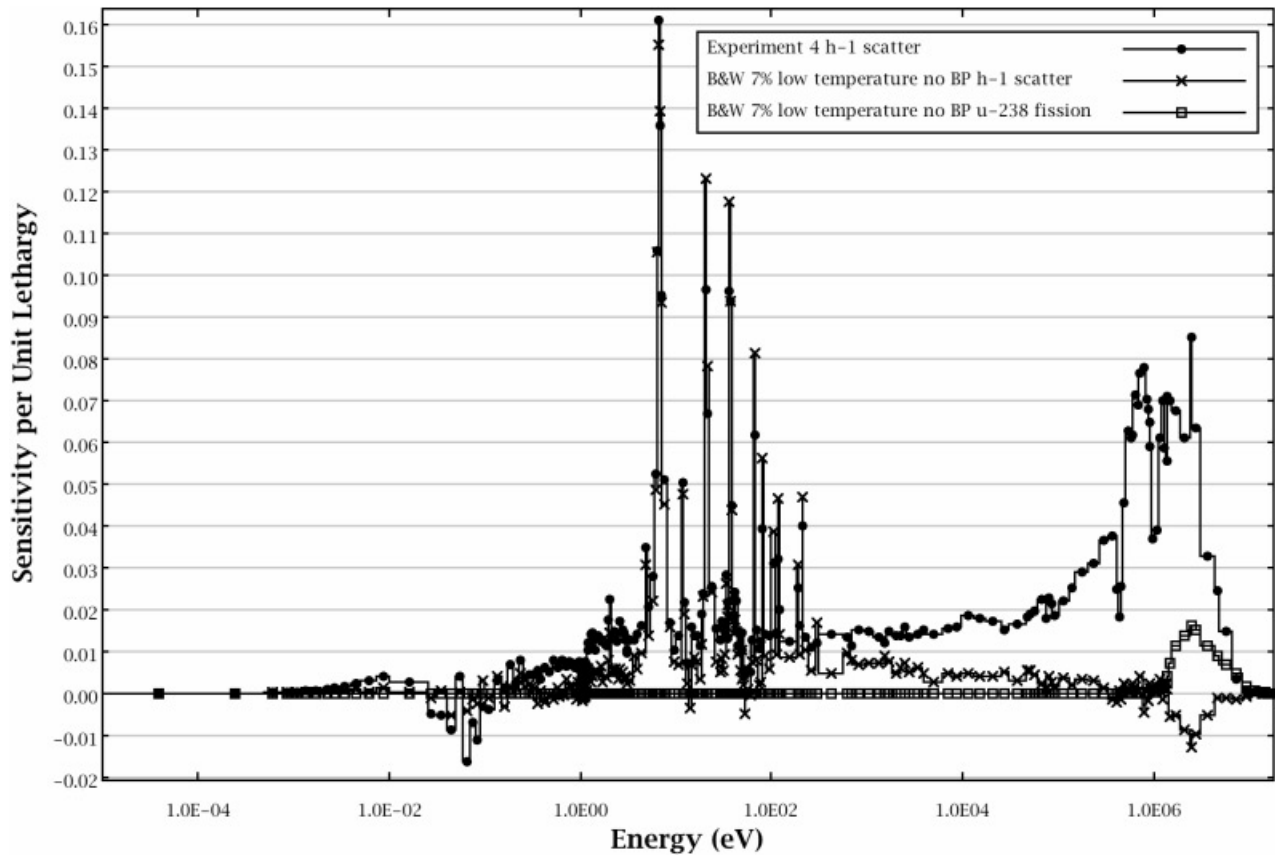


Fig. 18. Sensitivity of k_{eff} to the ^1H scatter cross section for proposed experiment 4 and ^1H scatter and ^{238}U capture cross sections for 7% enriched low-temperature B&W assembly with no BPs.

experiment 4 are shown in Table XVII. These results are similar to those for the 7% enriched low-temperature B&W assembly with no BPs and will not be discussed in detail.

For the 7% enriched low-temperature GE assembly with eight BPs, experiment 4 produces a c_k value of 0.89. The energy-integrated sensitivity coefficients for

this assembly and values of the g integral index in relation to experiment 4 are shown in Table XVIII. This assembly is more sensitive to ^{235}U fission, but the g value for ^{235}U fission is only 0.84. This is the primary cause of the lower-value c_k relative to the other systems investigated.

TABLE XVII
Nuclide-Reaction-Specific Analysis of Coverage Provided by Experiment 4 for 7% Enriched Low-Temperature Westinghouse Assembly with No BPs

	Fission		Capture		Scatter	
	Sensitivity	g	Sensitivity	g	Sensitivity	g
^1H			$-5.61\text{E}-02^a$	0.99	$1.14\text{E}-01$	0.89
^{16}O			$-4.29\text{E}-03$	0.65	$-2.65\text{E}-03$	0.75
Zr			$-5.81\text{E}-03$	0.0	$-3.53\text{E}-04$	0.0
^{235}U	$2.39\text{E}-01$	0.98	$-1.53\text{E}-01$	0.91	$1.44\text{E}-04$	0.68
^{238}U	$1.59\text{E}-02$	1.0	$-1.34\text{E}-01$	0.96	$9.33\text{E}-03$	0.86

^aRead as -5.61×10^{-2} .

TABLE XVIII
Nuclide-Reaction-Specific Analysis of Coverage Provided by Experiment 4 for 7% Enriched
Low-Temperature GE Assembly with Eight BPs

	Fission		Capture		Scatter	
	Sensitivity	<i>g</i>	Sensitivity	<i>g</i>	Sensitivity	<i>g</i>
¹ H			-1.06E-01 ^a	0.62	7.21E-02	0.79
¹⁶ O			-4.30E-03	0.65	-4.25E-03	0.70
Zr			-1.09E-02	0.0	-6.27E-04	0.0
¹⁵⁴ Gd			-1.04E-04	0.28	3.77E-07	0.23
¹⁵⁵ Gd			-6.44E-03	0.30	2.86E-06	0.24
¹⁵⁶ Gd			-3.62E-04	0.28	2.25E-05	0.26
¹⁵⁷ Gd			-1.45E-02	0.33	9.34E-06	0.28
¹⁵⁸ Gd			-1.91E-04	0.28	1.88E-06	0.23
¹⁶⁰ Gd			-4.72E-05	0.26	-1.73E-06	0.20
²³⁵ U	3.22E-01	0.84	-1.30E-01	0.93	-1.48E-04	0.47
²³⁸ U	2.04E-02	1.0	-1.08E-01	0.97	4.13E-03	0.770
Cr			-2.03E-04	0.27	-1.74E-06	0.26
Fe			-2.10E-04	0.69	-3.32E-06	0.44
Ni			-1.48E-04	0.0	-1.67E-06	0.0
¹¹² Sn			-2.31E-05	0.0	-1.10E-07	0.0
¹¹⁴ Sn			-5.13E-06	0.0	-1.05E-07	0.0
¹¹⁵ Sn			-7.36E-05	0.0	-5.65E-08	0.0
¹¹⁶ Sn			-1.08E-04	0.0	-6.28E-07	0.0
¹¹⁷ Sn			-1.62E-04	0.0	-1.32E-06	0.0
¹¹⁸ Sn			-1.11E-04	0.0	-1.07E-06	0.0
¹¹⁹ Sn			-9.60E-05	0.0	-1.48E-06	0.0
¹²⁰ Sn			-4.71E-05	0.0	-3.21E-06	0.0
¹²² Sn			-5.77E-06	0.0	-4.56E-07	0.0
¹²⁴ Sn			-2.83E-05	0.0	-6.02E-07	0.0
Hf			-6.88E-04	0.0	7.64E-08	0.0

^aRead as -1.06×10^{-1} .

IX. CONCLUSIONS

Conceptual designs for two series of proposed critical experiments using 6.93 wt% UO₂ fuel rods were presented. The intent of these proposed experiments is to provide validation data for reactor physics and criticality safety codes for the analysis of commercial power reactor fuels with enrichments ≥ 5 wt% ²³⁵U. TSUNAMI was used to analyze the applicability of the proposed experiments and 123 existing benchmark experiments to several prototypic commercial fuel designs.

Although the TSUNAMI analysis found several of the IHECSBE experiments to be applicable to each of the prototypic commercial fuel designs, none of the geometrical arrangements from these experiments reflect the geometrical arrangements of commercial reactor fuel and are not suitable for benchmarking computer codes commonly used to analyze commercial arrangements. Of the proposed experimental series, either of which adequately represents commercial reactor arrangements, the TSUNAMI analysis demonstrated that the square-design

configurations were the most applicable to the code validation of the prototypic commercial fuel designs. Because of the small size of the experimental core, the leakage of the experiment differs from that of an infinite array, leading to different sensitivities at fast energies. In the configurations of the proposed experiments containing BP rods, the importance of the Gd poison in the experiments does not equal that of an infinite array of poisoned assemblies but is similar to that of a simulated core where one-third of the assemblies contains BP rods. The square-design experiments provide the best data achievable from the project and will add significant new data for the validation of reactor physics and criticality safety codes, especially for PWR fuel designs with higher enrichments. The applicability of these experiments to BWR fuel designs with higher enrichments is somewhat limited but could be supplemented with subsequent experiments.

Additional research at ORNL is being conducted to extend the TSUNAMI techniques from eigenvalue perturbation theory to generalized perturbation theory. When

completed, sensitivity and uncertainty information could be computed for responses such as reaction rate ratios, control rod worths, and coolant void reactivity. Detailed assessments of experimental data to support the validation of these types of computations may be possible with advanced integral indices.

APPENDIX A

GLOBAL INTEGRAL INDEX

The mathematical development of the integral index c_k presented here is based on the development given in Ref. 3. The nuclear data parameters (i.e., groupwise nuclide-reaction-specific cross sections) are represented by the vector $\alpha \equiv (\alpha_m)$, $m = 1, 2, \dots, M$, where M is the number of nuclide-reaction pairs times the number of energy groups. The corresponding symmetric $M \times M$ matrix containing the relative variances (diagonal elements) and covariances (off-diagonal elements) in the nuclear data is

$$\mathbf{C}_{\alpha\alpha} \equiv \left[\frac{\text{COV}(\alpha_m, \alpha_p)}{\alpha_m \alpha_p} \right],$$

$$m = 1, 2, \dots, M; p = 1, 2, \dots, M, \quad (\text{A.1})$$

where

$$\text{COV}(\alpha_m, \alpha_p) = \langle \delta\alpha_m \delta\alpha_p \rangle, \quad (\text{A.2})$$

where $\delta\alpha_m$ and $\delta\alpha_p$ represent the difference between the values and expectation values of the nuclear data parameters and $\langle \rangle$ represents integration over the ranges of α_m and α_p weighted with a probability density function. A rigorous definition of the cross-section-covariance data is given in Ref. 9.

The matrix containing sensitivities of the calculated k_{eff} to the α parameters is given as

$$\mathbf{S}_{\mathbf{k}} \equiv \left[\frac{\alpha_m}{k_i} \frac{\partial k_i}{\partial \alpha_m} \right], \quad i = 1, 2, \dots, I; m = 1, 2, \dots, M, \quad (\text{A.3})$$

where I is the number of systems considered. The uncertainty matrix for the system k_{eff} values $\mathbf{C}_{\mathbf{k}\mathbf{k}}$, is given as

$$\mathbf{C}_{\mathbf{k}\mathbf{k}} = \mathbf{S}_{\mathbf{k}} \mathbf{C}_{\alpha\alpha} \mathbf{S}_{\mathbf{k}}^\dagger, \quad (\text{A.4})$$

where

\dagger = transpose

$\mathbf{S}_{\mathbf{k}}$ = $I \times M$ matrix

$\mathbf{C}_{\alpha\alpha}$ = $M \times M$ matrix

and the resulting $\mathbf{C}_{\mathbf{k}\mathbf{k}}$ matrix is of dimension $I \times I$. The $\mathbf{C}_{\mathbf{k}\mathbf{k}}$ matrix consists of relative variance values σ_i^2 for

each of the systems under consideration (the diagonal elements), as well as the relative covariance between systems σ_{ij}^2 (the off-diagonal elements). These off-diagonal elements represent the shared or common variance between two systems. The off-diagonal elements are typically divided by the square root of the corresponding diagonal elements (i.e., the respective standard deviations) to generate a correlation coefficient matrix. Thus, the correlation coefficient is defined as

$$c_k = \frac{\sigma_{ij}^2}{(\sigma_i \sigma_j)}, \quad (\text{A.5})$$

such that the single c_k value represents the correlation coefficient between uncertainties in systems i and j .

These correlations are primarily due to the fact that the uncertainties in the calculated k_{eff} values for two different systems are related since they contain the same materials. Cross-section uncertainties propagate to all systems containing these materials. Systems with the same materials and similar spectra would be correlated, while systems with different materials or spectra would not be correlated. The interpretation of the correlation coefficient is the following: A value of 0.0 represents no correlation between the systems, a value of 1.0 represents full correlation between the systems, and a value of -1.0 represents a full anticorrelation.

APPENDIX B

NUCLIDE-REACTION-SPECIFIC INTEGRAL INDEX

The nuclide-reaction-specific integral index g assesses the similarity of two systems based on normalized differences in the energy-dependent sensitivity data for a particular nuclide-reaction pair.⁸ The similarity measure used for g is based on the concept of coverage of the application by an experiment. A physical interpretation of the g index is the ratio of the sum of the sensitivity coefficients of the application that is covered by the experiment to the sum of the sensitivity coefficients for the application. The nuclide-reaction-specific integral index g , sometimes referred to as "little g ," is defined in terms of the normalized differences of the groupwise sensitivity coefficients for a particular nuclide n and reaction x summed over all energy groups j . Where the sensitivity of k_{eff} for an application system k_{eff}^a to a particular macroscopic cross-section data component $\Sigma_{x,j}^n$ is represented as

$$S_{x,j}^{a,n} \equiv \frac{\Sigma_{x,j}^n}{k_{eff}^a} \frac{dk_{eff}^a}{d\Sigma_{x,j}^n}$$

and where the sensitivity of k_{eff} for an experiment k_{eff}^e to the same macroscopic cross-section data component is represented as

$$S_{x,j}^{e,n} \equiv \frac{\sum_{x,j}^n \frac{dk_{eff}^e}{d\Sigma_{x,j}^n}}{k_{eff}^e},$$

the integral index g for reaction x of nuclide n is defined as

$$g_x^n = 1 - \frac{\sum_j (S_{x,j}^{a,n} - S_{x,j}^{e',n})}{\sum_j S_{x,j}^{a,n}}, \quad (\text{B.1})$$

where

$$S_{x,j}^{e',n} = \begin{cases} S_{s,j}^{e,n}, & \text{where } |S_{x,j}^{a,n}| \geq |S_{x,j}^{e,n}| \text{ and } \frac{S_{x,j}^{a,n}}{|S_{x,j}^{a,n}|} = \frac{S_{x,j}^{e,n}}{|S_{x,j}^{e,n}|} \\ S_{x,j}^{a,n}, & \text{where } |S_{x,j}^{a,n}| < |S_{x,j}^{e,n}| \text{ and } \frac{S_{x,j}^{a,n}}{|S_{x,j}^{a,n}|} = \frac{S_{x,j}^{e,n}}{|S_{x,j}^{e,n}|} \\ 0, & \text{otherwise} \end{cases},$$

and the j summation is performed over all energy groups.

The definition of $S_{x,j}^{e',n}$ restricts the coverage of the application by the experiment to the portion of the experiment's sensitivity coefficient that does not exceed that of the application in magnitude. Additionally, the application's sensitivity coefficient and that of the experiment must have the same sign. The use of 1 minus the normalized difference makes the range of this index consistent with other integral indices in TSUNAMI-IP, including C_k . The g index is normalized such that a g value of 1 indicates complete coverage of the application by the experiment for the particular nuclide-reaction pair. A g value of 0 indicates no coverage of the application by the experiment for the particular nuclide-reaction pair.

ACKNOWLEDGMENTS

This work was performed as part of DOE NERI project 2001-0124 under contract DE-FG07-01SF22330. The authors acknowledge M. A. Feltus of DOE for her assistance in many aspects of this project. The authors also acknowledge J. S. Tulenko and R. M. Smith of UF; M. Pitts, M. Saglam, and D. Dziadosz of Framatome ANP; and C. V. Parks of ORNL for their assistance with the design and/or support of the analysis work in this project. The authors also acknowledge J. C. Wagner and C. O. Slater of ORNL, R. A. Kockendarfer and T. A.

Coleman of Framatome ANP for their review of this manuscript, and J. B. Anderson and S. L. Parker of ORNL for their editorial assistance. Framatome ANP is an AREVA and Siemens Company. ORNL is managed by UT-Battelle, LLC, for the DOE under contract DE-AC05-00OR22725.

REFERENCES

1. "Specification for Uranium Dioxide Pellets," Spec. No. 41-1001, Allis-Chalmers Manufacturing Company, Atomic Energy Division (1965).
2. G. A. HARMS, P. H. HEMMICK, J. T. FORD, S. A. WALKER, D. T. BERRY, and P. S. PICKARD, "Experimental Investigation of Burnup Credit for Safe Transport, Storage, and Disposal of Spent Nuclear Fuel," SAND2004-0912, Sandia National Laboratories (2004).
3. B. L. BROADHEAD, B. T. REARDEN, C. M. HOPPER, J. J. WAGSCHAL, and C. V. PARKS, "Sensitivity- and Uncertainty-Based Criticality Safety Validation Techniques," *Nucl. Sci. Eng.*, **146**, 340 (2004).
4. B. T. REARDEN, "Perturbation Theory Eigenvalue Sensitivity Analysis with Monte Carlo Techniques," *Nucl. Sci. Eng.*, **146**, 367 (2004).
5. "SCALE: A Modular Code System for Performing Standardized Computer Analyses for Licensing Evaluation," NUREG/CR-0200, Rev. 7 (ORNL/NUREG/CSD-2/V1/R7), Oak Ridge National Laboratory (June 2004).
6. K. R. ELAM and B. T. REARDEN, "Use of Sensitivity and Uncertainty Analysis to Select Benchmark Experiments for the Validation of Computer Codes and Data," *Nucl. Sci. Eng.*, **145**, 196 (2003).
7. "International Handbook of Evaluated Criticality Safety Benchmark Experiments," Nuclear Energy Agency Nuclear Science Committee of the Organization for Economic Co-operation and Development, NEA/NSC/DOC(95)03, Nuclear Energy Agency (2003).
8. S. GOLUOGLU, C. M. HOPPER, and B. T. REARDEN, "Extended Interpretation of Sensitivity Data for Benchmark Areas of Applicability," *Trans. Am. Nucl. Soc.*, **88**, 77 (2003).
9. M. E. DUNN, "PUFF-III: A Code for Processing ENDF Uncertainty Data Into Multigroup Covariance Matrices," ORNL/TM-1999/235 (NUREG/CR-6650), U.S. Nuclear Regulatory Commission/Oak Ridge National Laboratory (2000).